GRS evidence and the possibility of paleooceans on Mars

James M. Dohm [a,b,*], Victor R. Baker [a,b], William V. Boynton [b], Alberto G. Fairén [c], Justin C. Ferris [d], Michael Finch [b], Roberto Furfaro [e], Trent M. Hare [f], Daniel M. Janes [b], Jeffrey S. Kargel [a], Suniti Karunatillake [g], John Keller [h], Kris Kerry [b], Kyeong J. Kim [i], Goro Komatsu [j], William C. Mahaney [k,l], Dirk Schulze-Makuch [m], Lucia Marinangeli [j], Gian G. Ori [j], Javier Ruiz [n], Shawn J. Wheelock [a]

[a] *Department of Hydrology and Water Resources, University of Arizona, Tucson, AZ 85721, USA*
[b] *Lunar and Planetary Laboratory, University of Arizona, Tucson, AZ 85721, USA*
[c] *Space Science and Astrobiology Division, NASA Ames Research Center, Moffett Field, CA 94035, USA*
[d] *California Water Science Center, US Geological Survey, Sacramento, CA 95819, USA*
[e] *Aerospace and Mechanical Engineering Department, University of Arizona, Tucson, AZ 85721, USA*
[f] *United States Geological Survey, Flagstaff, AZ 86001, USA*
[g] *Center for Radiophysics and Space Research, Cornell University Ithaca, NY 14853, USA*
[h] *Department of Physics, California Polytechnic University, San Luis Obispo, CA 9340, USA*
[i] *Geological and Environmental Hazards Division, Korea Institute of Geosciences and Mineral Resources, Daejeon, South Korea*
[j] *International Research School of Planetary Sciences, Università d'Annunzio, Pescara, Italy*
[k] *Geomorphology and Pedology Laboratory, York University, Atkinson College, Ontario, Canada M3J 1P3*
[l] *Quaternary Surveys, Thornhill, Ontario, Canada L4J 1J4*
[m] *School of Earth and Environmental Sciences, Washington State University, Pullman, WA 99164, USA*
[n] *Museo Nacional de Ciencias Naturales, CSIC, José Gutiérrez Abascal 2, 28006 Madrid, Spain*

ARTICLE INFO

Article history:
Received 15 February 2008
Received in revised form
14 August 2008
Accepted 7 October 2008
Available online 29 October 2008

Keywords:
Mars
Gamma-ray spectrometer
Oceans
Water
Elemental
Hydrogeology

ABSTRACT

The Gamma Ray Spectrometer (Mars Odyssey spacecraft) has revealed elemental distributions of potassium (K), thorium (Th), and iron (Fe) on Mars that require fractionation of K (and possibly Th and Fe) consistent with aqueous activity. This includes weathering, evolution of soils, and transport, sorting, and deposition, as well as with the location of first-order geomorphological demarcations identified as possible paleoocean boundaries. The element abundances occur in patterns consistent with weathering *in situ* and possible presence of relict or exhumed paleosols, deposition of weathered materials (salts and clastic minerals), and weathering/transport under neutral to acidic brines. The abundances are explained by hydrogeology consistent with the possibly overlapping alternatives of paleooceans and/or heterogeneous rock compositions from diverse provenances (e.g., differing igneous compositions).

1. Introduction

A large and somewhat confusing body of literature has developed on the question of whether water bodies ranging in scale from oceans to lakes ever occupied the northern plains of Mars, primarily through Viking-based geomorphic investigation (e.g., Jöns, 1986; Lucchitta et al., 1986; Parker et al., 1987, 1989, 1993; Baker et al., 1991; Goldspiel and Squyres, 1991; Scott et al., 1995). The confusion may be attributed to several factors including the possibility that these putative water bodies were not necessarily Earth-like and thus may leave different markers in the geologic record (see Section 2). In addition, there is a lack of consistency in describing paleoocean boundaries by various investigators. For example, the term contact and shoreline have been used to describe a possible paleoocean boundary, hypothesized mainly through geomorphology and topography. Hereafter, we will use the term paleoocean boundary rather than using qualifiers such as possible, putative, or hypothesized.

More recently, analyses of Mars Orbiter Laser Altimeter (MOLA) topography supported the existence of a paleoocean (Head et al., 1998, 1999). However, an investigation using Mars Orbiter Camera (MOC) and Thermal Emission Imaging System (THEMIS) image data could not confirm the proposed local paleoocean boundaries (Malin and Edgett, 1999, 2001; Ghatan and Zimbelman, 2006). Nevertheless, subsequent geologic investigation indicated several episodes of water inundation in the

* Corresponding author at: Department of Hydrology and Water Resources, University of Arizona, Tucson, AZ 85721, USA. Tel.: +1 520 6268454; fax: +1 520 6211422.
E-mail address: jmd@hwr.arizona.edu (J.M. Dohm).

northern plains, which includes the formation of water bodies ranging from lakes to oceans, beginning in the Noachian and occurring both in the Hesperian and Amazonian, primarily related to Tharsis-induced flooding (see Fairén et al. (2003) that details the hypothesized paleohydrological events). Endogenic-driven paleohydrologic activity is also reported to have included spring-fed activity (e.g., Tanaka et al., 2003, 2005), acidic aqueous conditions (Fairén et al., 2004), and transient wetter climatic periods (Baker et al., 1991).

Results from the most recent decade of Mars' missions highlight a water- and ice-sculpted Martian landscape. Evidence includes layered sedimentary sequences with weathered outcrops, debris flows and both small and large fluvial valleys, alluvial fans, fluvial-lacustrine deltas (Malin and Edgett, 2000, 2003; Edgett and Malin, 2002, 2003; Edgett, 2005), glacial and periglacial landscapes (Head and Pratt, 2001; Kargel, 2004; Head et al., 2006a, b; Kostama et al., 2006; Soare et al., 2007), and geochemical/mineralogical signatures of aqueous weathering, iron accumulation on older surfaces, leaching, and deposition, such as sulfates (Gendrin et al., 2005) and clays (Fialips et al., 2005). Such evidence indicates weathered zones and possible paleosols in stratigraphic sequences (e.g., Mahaney et al., 2001), transport of water and rock materials to sedimentary basins (e.g., Dohm et al., 2001a, 2007a), and the formation of extensive lakes (e.g., Scott et al., 1995; Cabrol et al., 2001) and possibly transient oceans (e.g., Fairén et al., 2003; Greenwood and Blake, 2006) on Mars. This new evidence is consistent with Viking-era geologic investigations that reported hydrogeologic activity and inferred episodic climate change occurring at intervals from the Noachian into recent geologic times, well into the Amazonian period (e.g., Scott et al., 1995), consistent with the MEGAOUTFLO hydrologic model of Mars (Baker et al., 1991, 2000). It may even indicate aqueous activity at present (Ferris et al., 2002; Miyamoto et al., 2004; Malin et al., 2006). Abundance of water and dynamic activity would be decisively important for the possibility of past and present life on Mars (e.g. Schulze-Makuch and Irwin, 2004; Schulze-Makuch et al., 2005a).

The deficiency of carbonates present at the Martian surface has been claimed as evidence that aqueous activity was sharply limited on Mars and that ocean-scale hydrology could not have occurred (e.g., Carr and Head, 2003). This interpretation has been countered by a case made for possible acid–sulfate aqueous conditions (Fairén et al., 2004; Greenwood and Blake, 2006), which would have precipitated gypsum, jarosite, and other sulfate minerals rather than carbonates, such as calcite and dolomite; this would include oxidizing conditions (e.g., Fe^{3+}) that would drive the formation of hematite and acidic solutions from which jarosite is expected to form at pH ~2 (boundary of jarosite; Fairén et al. (2004)). This case was later strengthened by the Mars Exploration Rover (MER) Opportunity-based identification of jarosite-bearing stratigraphic sequences (Squyres et al., 2004) and by the discovery of gypsum, kieserite, and polyhydrated sulfates at the MER landing sites and also found by Mars Express OMEGA at locations scattered across Mars (Gendrin et al., 2005; Bibring et al., 2006).

Here, we present the results of comparative analyses of Mars Odyssey Gamma Ray Spectrometer (GRS)-based potassium (K), thorium (Th), and iron (Fe) map information (recorded in rock materials up to 0.33 m depth; see Section 3) with topography and reported paleoocean-boundary information in order to add new insight on the ongoing debate. Since GRS detects gamma rays from the surface at a spatial resolution approximately equal to the altitude of the spacecraft of ~450 km (Boynton et al., 2004, 2006), we assume that the regional variations in compositions of the upper crust are manifested in the observed patterns of element concentrations by global to regional geological and paleohydrological processes. These may include igneous activity, surface and subsurface water flow and ponding, and ice-related processes (Scott and Tanaka, 1986; Kargel and Strom, 1992; Soare et al., 2007). Presumably there are local overprints by eolian materials and other veneers, but the operative assumption is that these surficial veneers were either derived locally or cover small enough fractions of the surface that they do not obscure the composition represented by the deeper geology. Because of the well-known major roles of shallow ground ice and seasonal carbon dioxide frost veneers at high latitudes, our analysis is truncated at ±50–60° latitude (Boynton et al., 2007). Our results are consistent with aqueous conditions described above including the formation of bodies of standing water in the northern plains (including both oceans and lakes; Scott et al., 1995; Fairén et al., 2003). There are other hydrochemical explanations, as we describe below, but also of consideration is that if meteoric water existed in an oxygen-rich atmosphere, paleosols must exist in the Martian environment, albeit likely mantled in many cases (see Mahaney et al. (2001) for an Earth analogue). Igneous processes may have achieved comparable fractionation of K, Th, and Fe (Taylor et al., 2006a; Karunatillake et al., 2006) and would not necessarily carry any climatic and volatile implications, but igneous processes alone would not fit well with the emerging model of a hydrologically and hydrochemically active Mars. The model of K fractionation controlled, in part, by global hydrology and water bodies ranging in size from lakes to oceans lends itself to a set of specific, powerful, and testable predictions such as the presence of basins with wide lateral and vertical zonation of clastic and chemical mineral facies. Next, we discuss why water bodies such as oceans may not distinctly leave an Earth-like geomorphic mark (but not dismissing lakes that have been reported to have occurred in parts of the northern plains during the Amazonian period (e.g., Scott et al., 1995)), subsequent to detailing the GRS signatures and their implications on whether such water bodies may have existed on Mars.

2. Considerations for paleoocean-boundary demarcations on Mars

Despite a lack of incontrovertible evidence that the Martian surface was covered by an ocean, a collection of geomorphic and geologic evidences point to the existence of transient water bodies (Scott et al., 1995; Fairén et al., 2003). The term "ocean" has been applied to the larger of these (e.g., see shoreline demarcations based from Fairén et al. (2003) in Fig. 1). Although initially inferred from sedimentary landforms on the northern plains (e.g., Jöns, 1986; Lucchitta et al., 1986) and later from global hydrologic considerations (e.g., Gulick and Baker, 1990; Baker et al., 1991), oceans have been most controversially tied to the identification of "shorelines" made by Parker et al. (1987, 1989, 1993). For example, Parker et al. (1993) described seven different boundaries, but only two of them could be approximately traced as complete closures within and along the margins of the northern lowlands. Parker et al. (1993) proposed an outer boundary, which they referred to as Contact 1 (and renamed as Arabia shoreline by Clifford and Parker (2001)), located along the Martian highland-lowland boundary (as the high water mark of a primitive ocean), and a younger enclosure inset within the more extensive outer boundary, which in turn they referred to as Contact 2 (also named Deuteronilus shoreline by Clifford and Parker (2001), or Shoreline 2 by Fairén et al. (2003)).

Subsequent analyses by Head et al. (1998, 1999) and Carr and Head (2003), however, pointed out that the younger boundary might represent the only true paleoocean demarcation, because the variations of the elevation in the older boundary do not reflect an equipotential surface. This consideration, however, did not take

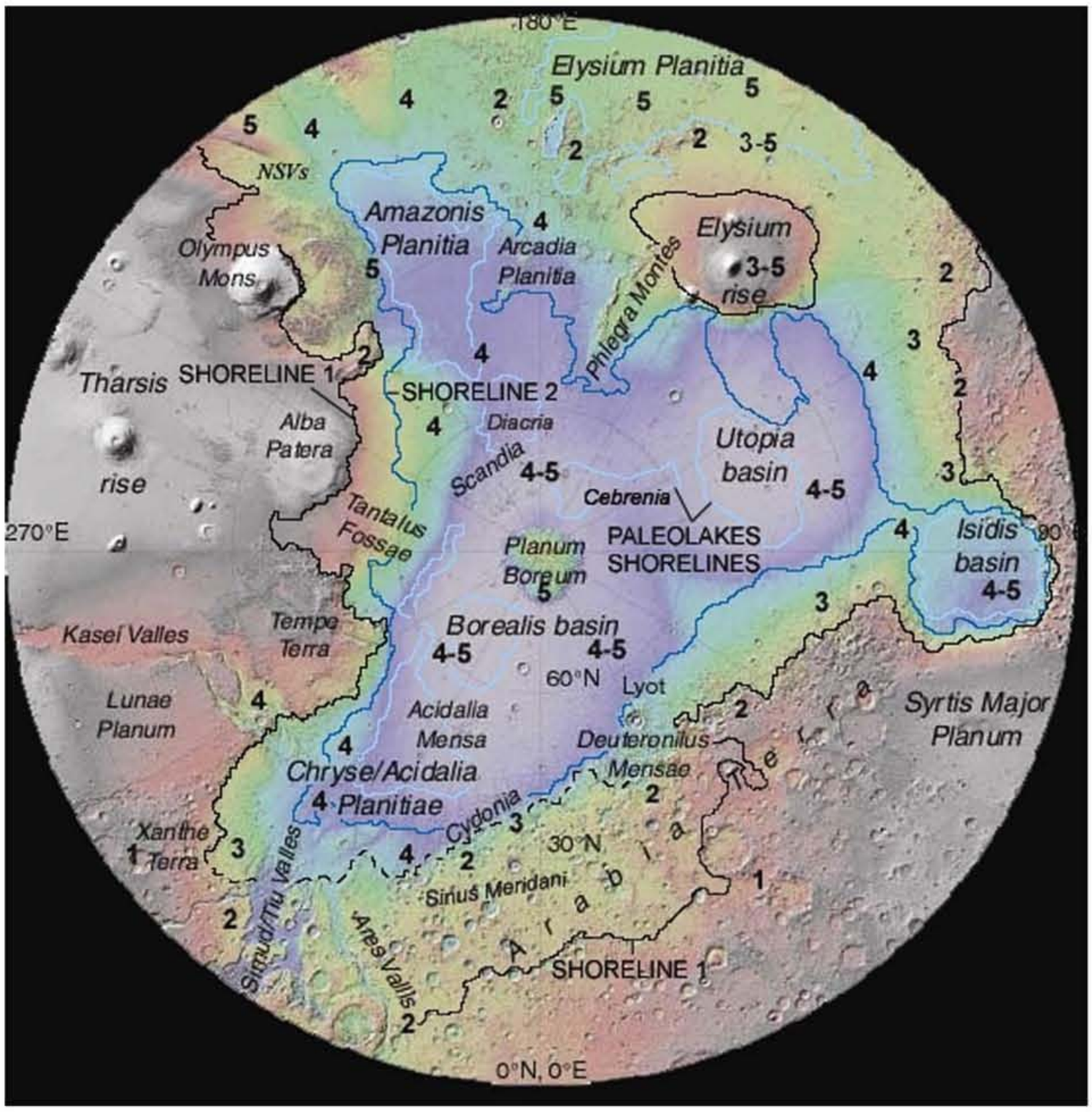

Fig. 1. After Fairén et al. (2003), topographic shaded relief map of the northern hemisphere of Mars constructed from MOLA data showing major geographic features of the northern hemisphere, including three major basins (Borealis basin = Vastitas Borealis, Utopia basin = Utopia Planitia, Isidis basin = Isidis Planitia). Also shown are Revised Shoreline 1 (RS1; black line *referred to here as older paleoocean boundary*), Shoreline 1 (dashed-black line) and Shoreline 2 (dark blue line *referred to here as younger paleoocean boundary*), which are based on Edgett and Parker (1997), Carr (2002), Parker et al. (1987, 1989, 1993, 2001) and Head et al. (1999); paleolakes (light blue line), based on Scott et al. (1995); and Stage information (numbers) that reflects the geologic mapping of Tanaka et al. (2003) and correlative with Stage information of Dohm et al. (2001a, c) and Anderson et al. (2001). Polar Stereographic projection; scale varies with latitude; modified from Tanaka et al., (2003). Please see color version online.

into account the distinction between present-day topography and paleotopography. Indeed, it is not necessarily true that a paleoequipotential surface implies a good fit to a present-day equipotential surface. Several processes could significantly deform the original long-wavelength topography of Martian paleoocean boundaries following the disappearance of the possible oceans. Different thermal histories among Martian regions could produce elevation differences of kilometer scale through thermal isostasy, even for initial variations in surface heat flow of relative amplitude similar to those in tectonothermally stable terrestrial continental areas (Ruiz et al., 2004). Lithospheric rebound due to water unloading associated with the disappearance of an ocean with irregularly shaped margins could result in deviations of equipotentiality of up to several hundreds of meters (Leverington and Ghent, 2004). Changes in the orientation of the rotation axis, maybe associated with the emplacement and removal of oceans, may induce perturbations of the centrifugal potential, and hence in the surface topography (Perron et al., 2007). Martian paleoocean boundaries could fit paleoequipotential surfaces if the reference ellipsoid for the planet has changed with time, possibly due to the formation of Tharsis (Sotin and Couturier, 2007). Moreover, a revision by Ruiz et al. (2003, 2006) and Fairén et al. (2003) to the older paleoocean demarcation initially defined by Parker et al. (1987, 1989, 1993) and Clifford and Parker (2001), makes the older paleoocean more expansive, transecting the Meridiani, Arabia, Utopia, Elysium, and Amazonis regions. This revised, more extensive, older paleoocean boundary is closer to a paleoequipotential surface than the previously proposed demarcation (López et al., 2006; Ruiz et al., 2006). In this work, the older boundary is therefore equivalent to this revised demarcation and the younger boundary is equivalent to the previously reported younger paleoocean demarcation (e.g., "Shoreline 2" in Fairén et al., 2003).

Failure to confirm certain "shoreline" landforms locally on MOC and THEMIS imagery is a weakness of the ocean hypothesis (Malin and Edgett, 1999, 2001; Ghatan and Zimbelman, 2006), though it does not invalidate the entire hypothesis of plains oceans. An often neglected detail in existing literature is that Mars lacks a sizable Moon. The distinct geomorphic features formed at the coasts of terrestrial large lakes and oceans are largely a direct result of the enormous tidal energy imparted by the Moon. In addition, whereas many coastal landforms as we see on Earth (e.g., barrier islands, spits, and bars) would be prone to eolian reworking, burial, or obliteration unless the landform became lithified, erosion/burial alone seems an inadequate explanation for the absence of these classic landform types (Tanaka et al., 2003). Inundation of the northern plains could have taken the form largely of giant debris flows and liquefied sediments (Jöns, 1986), which would not have produced the type of marine coastal landforms some people had expected to see. The oceans may have

also been ice-covered (e.g., Kargel et al., 1995; Kreslavsky and Head, 2002), which would prevent wave action. The ice cover would influence near-coastal erosion, deposition, and therefore the geomorphological signature of ocean margins. Finally, in many areas, the ocean itself may still exist as a still-frozen, partially sublimated, debris-laden mass of ice, and this of course would obscure seafloor landforms right up to the margins of the frozen bodies. For example, the Cerberus plains has been recently identified as a frozen sea based on the Mars Express high-resolution stereo camera (Murray et al., 2005), while another interpretation includes flood volcanism (e.g., Plescia, 1990), including lava-ice interaction (Lanagan et al., 2001; Fagents et al., 2002). Free-air gravity data indicate large gravity lows (−100 to −200 mGal) across much of the northern plains, notably in the basins where the circum-Chryse channels debouched (Fig. 2).

The MGS data confirms the initial observations of a regional mantling layer of sediment, referred to as the Vastitas Borealis Formation during Viking-era geologic investigations (Scott and Tanaka, 1986; Tanaka, 1986; Greeley and Guest, 1987), covering perhaps 3×10^7 km^2 of the northern plains (Head et al., 2002). The outer contact of the Vastitas Borealis Formation is approximately coincident with the trace of the younger paleoocean boundary in the Deuteronilus, Nilosyrtis, Isidis, Tempe, and Chryse regions (see Carr and Head, 2003). This massive deposit is contemporaneous with Late Hesperian/Early Amazonian outflow-channel development, and it was likely emplaced as the sediment-laden outflow-channel discharges became hyperpycnal flows upon entering water ponded on the plains (Ivanov and Head, 2001). Spring-fed activity has also been proposed to have contributed to the regionally extensive deposit (Tanaka et al., 2005). In another scenario, Clifford and Parker (2001) envision a Noachian "ocean," contemporaneous with the widespread formation of valley networks in the southern cratered highlands, fed by a great fluvial system extending from the south polar cap through Argyre and

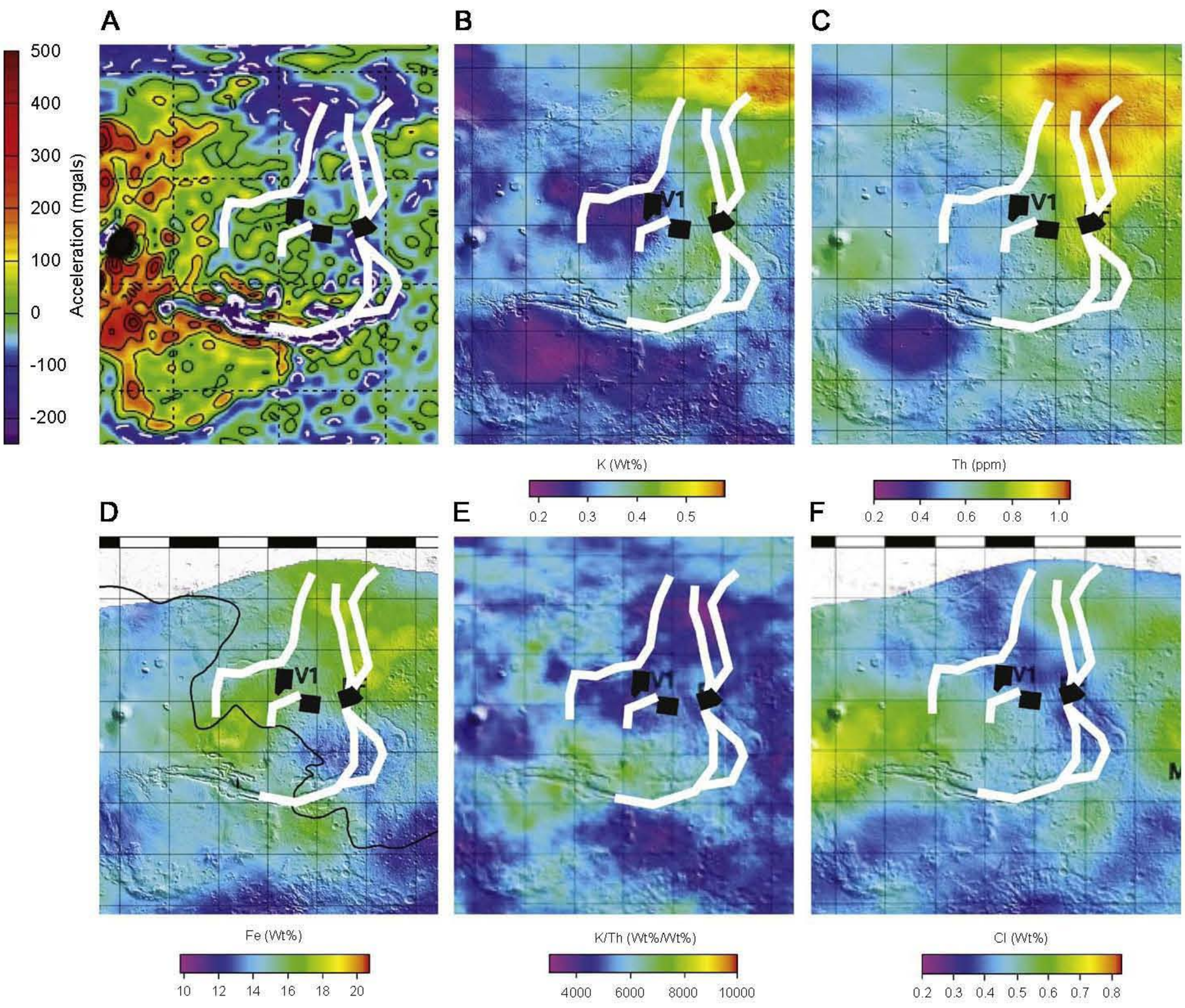

Fig. 2. (A) Gravity-low patterns (white lines) and highly degraded Chryse impact rim (black dashed line) annotated on free-air surface anomalies of the MGS95J gravity model to degree and order 70 (Konopliv et al., 2006). The gravity-low anomaly patterns generally correspond with major drainage pathways of the circum-Chryse outflow channel system. Though the interpretation of gravity anomalies is neither unique nor simple, as gravity anomalies can either be positive or negative due to several factors including whether sedimentary materials are ice-rich or not and whether the deposit were emplaced prior to or following compensation, noteworthy is that the outflow channel spillway zone of Acidalia Planitia is a striking negative anomaly which correlates with the anomalous elevated K and Th regions of (B) and (C). Iron also appears to be elevated in the spillway zone (D). Both K/Th (E) and Cl appear low to moderate, respectively.

the Chryse Trough, to the northern plains. For example, the elevation of the base levels of the Chryse outflow channels is close to the mean level of the younger paleoocean boundary, which could indicate that they debouched into a large standing body of water (Head et al., 1999; Ivanov and Head, 2001).

Baker et al. (1991) first proposed a linkage among Tharsis-sourcing endogenic heat release, volatile outbursts including flooding, and ponding in the northern plains to form *Oceanus Borealis* (Fig. 3). Such a linkage, later referred to as the MEGAOUTFLO model (Baker et al., 2002, 2007), ascribes the episodic formation of *Oceanus Borealis* on the northern plains of Mars as one component of a cycle. Phenomenally long post-heavy-bombardment epochs during which the Martian surface had extremely cold and dry conditions, are punctuated by short-duration ($\sim 10^4$–10^5 year) episodes of quasi-stable conditions. These shorter periods would be considerably wetter and somewhat warmer than those prevailing today at the planet's surface. In this model, the transition from the persistent cold–dry state to the warm–wet state (approximating Antarctic and London fog conditions) are initiated by cataclysmic flood outbursts from the Martian outflow channels. On the other hand, hypothesized changes in planetary obliquity in the Late Amazonian would necessarily redistribute moisture, resulting in the resurfacing of some northern plains materials (e.g., Head et al., 2006a, b; Forget et al., 2006; Soare et al., 2007).

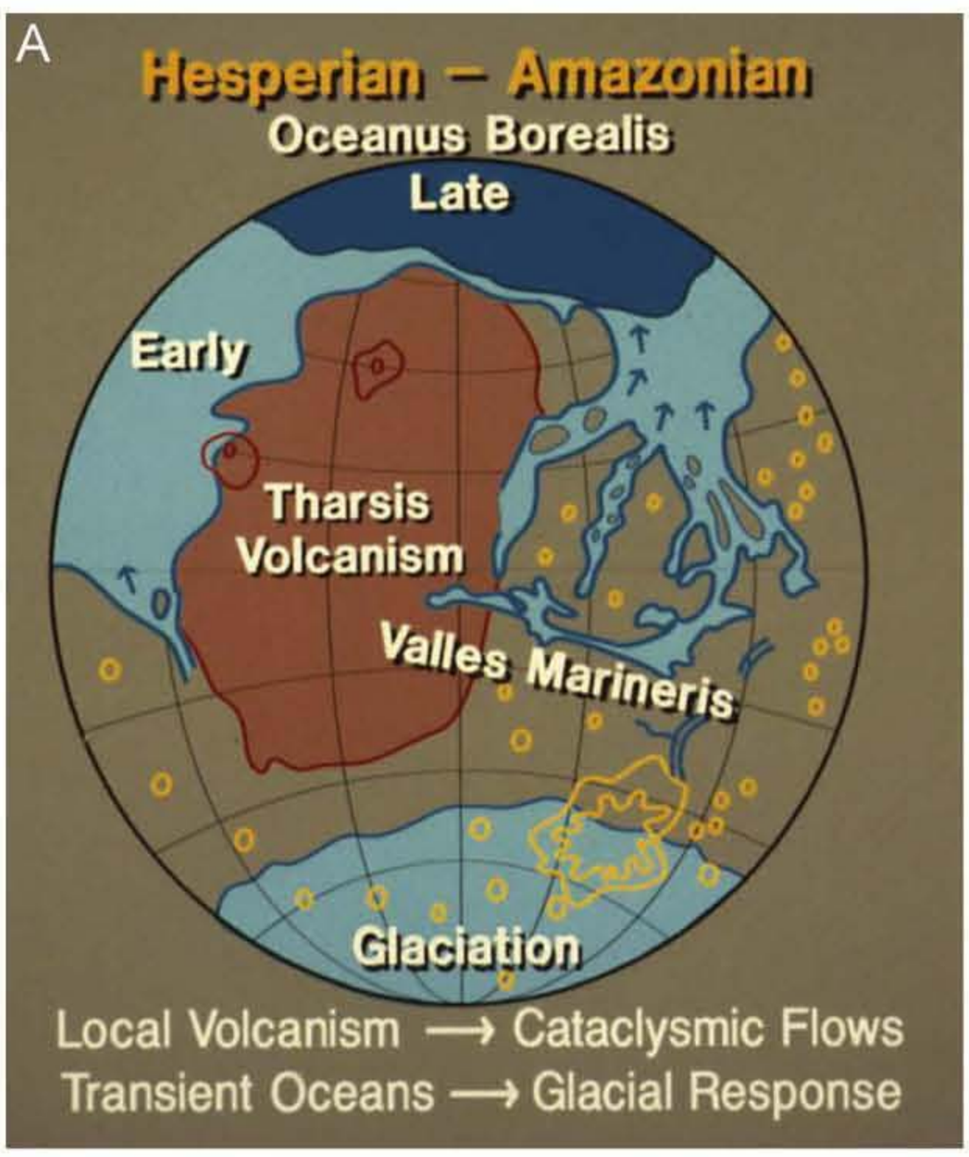

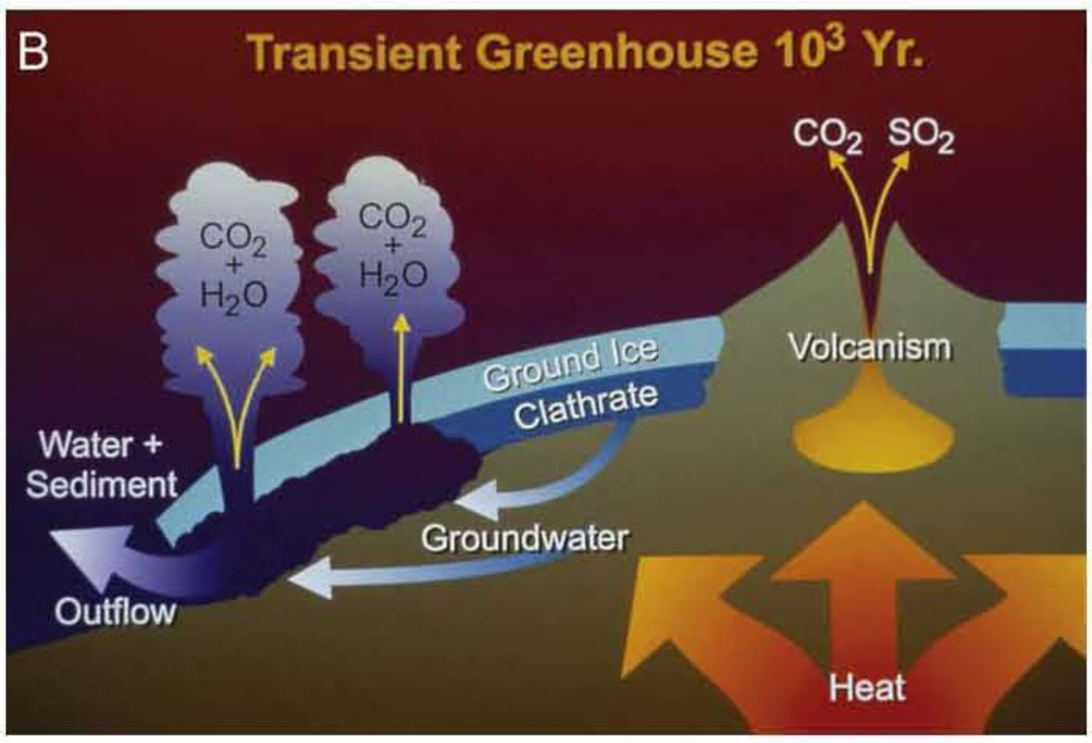

Fig. 3. (a, b) A genetic model, MEGAOUTFLO, first presented in 1991, ascribes the episodic formation of the possible Oceanus Borealis to cataclysmic outburst flooding of the outflow channels, driven by Tharsis activity, and release of other volatiles to result not only in oceans but also transient climatic perturbations, which includes glaciation (e.g., Kargel and Strom, 1992). Please see color version online.

Consistent with the MEGAOUTFLO hypothesis, geologic investigation (including analyses of stratigraphic, paleotectonic, geomorphologic, and topographic information) revealed a linkage between major stages of Tharsis activity (Dohm et al., 2001a, b, 2007b; Anderson et al., 2001), as well as the Elysium rise (to a lesser extent; e.g., Tanaka et al., 2005), and northern plains inundations (Fairén et al., 2003). Among the water bodies originated by these inundations was at least one great Noachian-Early Hesperian northern plains ocean covering approximately $\frac{1}{3}$ of the planet's surface, a Late Hesperian sea inset within the margin of the high water marks of the previous ocean, and widely distributed minor lakes that may represent a reduced Late Hesperian sea with ponded waters in the deepest parts of the northern plains (Fairén et al., 2003; Fig. 1).

Based on the possible occurrence of water bodies ranging from oceans to lakes in the northern plains over relatively long time periods, a preliminary assessment for marine-target impact craters identified candidates that resemble their terrestrial counterparts (Ormö et al., 2004a). A relatively large (e.g., tens of kilometers in diameter) impact would generate an immense tsunami in such a comparatively shallow sea. If even *one* such event occurred during the period of maximum oceanic extent, the resultant series of waves would have traversed the entire ocean, delivering their kinetic energy almost entirely at the shore. The powerful, chaotic series of waves would effectively erase terraces, barrier islands, and other formations that we associate with large, terrestrial bodies of water. In their place, one would likely find an entirely different set of geomorphic features, such as back flow channels from where the waters returned to the basin (Ormö et al., 2004a). Such an event would help explain, in part, why the previously mentioned geomorphic expression of paleoocean-boundary demarcations appear heavily muted at the limits of our current observational technologies.

In addition to water and rock materials being transferred from the highlands to the lowlands during the hypothesized internally driven events, elements may have been leached from weathering mantles or paleosols in the highland materials and concentrated in the lowlands, since at least part of this recorded aqueous history included acidic conditions (Fairén et al., 2004; Fig. 4). Another possibility is that the movement of Fe from the highlands to the lowlands could include substitution of Fe for Al in the clay mineral lattice such as in the case kaolinite, halloysite, or illite followed by clay transport; the GRS-based Al map, which is currently under preparation, will help address this potential. Though this may be a better way to explain Fe increase in the lower sites, wind could transport larger grains, accumulating Fe in the basins. The acidic aqueous conditions described above were hypothesized to precipitate jarosite and inhibit carbonates from forming at and near the surface of Mars (Fairén et al., 2004). This was confirmed by the MER Opportunity (Squyres et al., 2004). In addition, goethite has been suggested through MER Spirit-based exploration, also consistent with low-pH aqueous alteration (Ming et al., 2006). The position of the Noachian paleoocean boundary, which covered about $\frac{1}{3}$ of the planet's surface, was mapped as being topographically higher than Opportunity's current position (Fairén et al., 2003). It is also reported to have occurred when conditions on Mars may have approximated Earth-like Archean conditions (Baker et al., 2002, 2007; Fairén and Dohm, 2004;

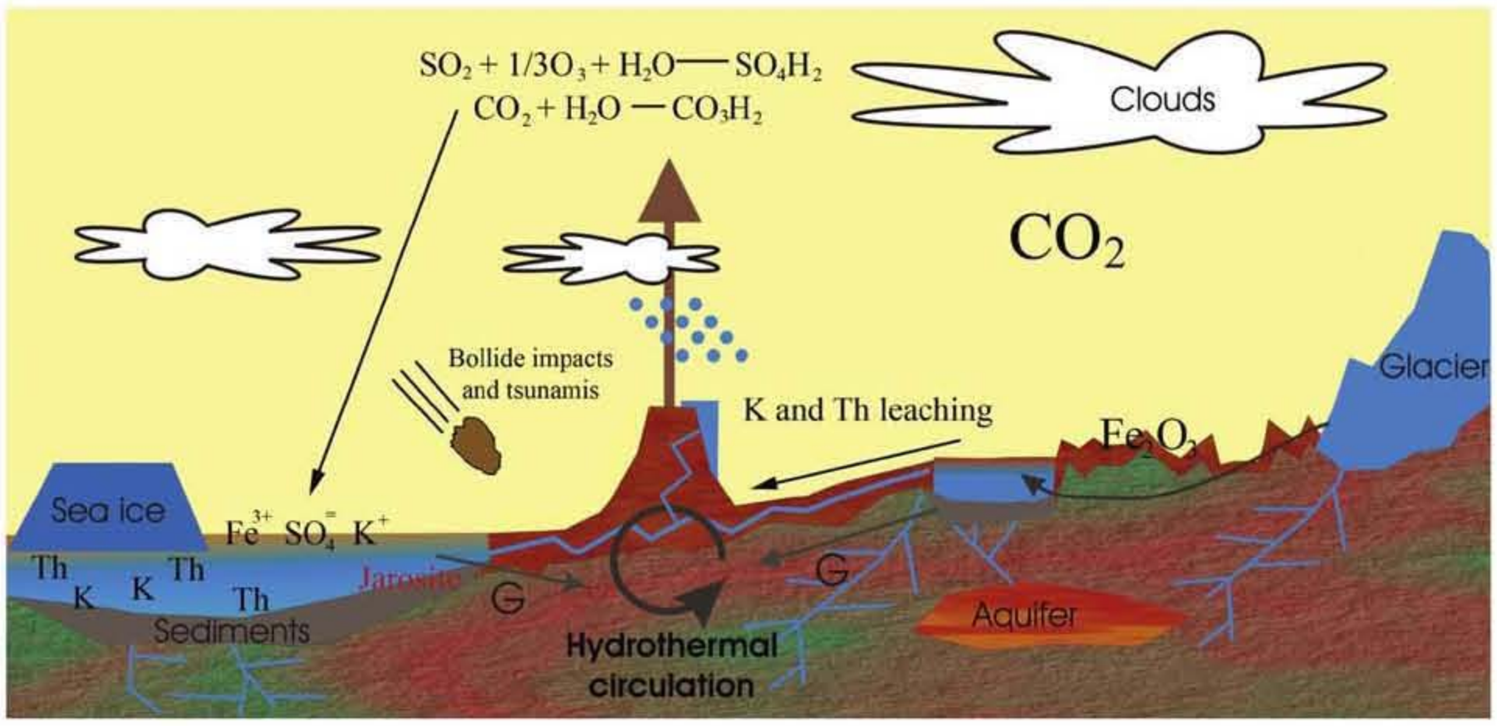

Fig. 4. Schematic representation of land–ocean–atmosphere interactions associated with the presence of a long-term hydrological cycle and induced acidic environments during early Mars. The acidic attack of ultramafic crust is driven by H_2SO_4 and H_2CO_3, and consequently weathering of basalt releases Fe and Mg to the sea water. From these solutions, jarosite as well as Mg sulfates are expected to precipitate, as highlighted by MER Opportunity at Meridiani. On the other hand, rock materials such as igneous phosphatic pegmatites include monazite as a component, which is ultimately weathered out from the host rock and carried downstream great distances and eventually collect in river deposits and even in ocean beach deposits, leaving behind the Th signature. On the other hand, acidic aqueous conditions can leach mobile K and less mobile Th from highland rock materials, which are subsequently transported down gradient through hydrologic processes, concentrating in the northern plains. G: Groundwater flow systems recharge. Please see color version online.

Schulze-Makuch et al., 2005a, b). Following the formation of the highland–lowland boundary, acidic aqueous conditions may have resulted in a transferal of elements from the highlands to the lowlands. Such a transfer would concentrate soluble elements such as K and Th below an equipotential surface (e.g., a paleoocean boundary). Due to their varying mobility, K, Th, and their ratio are often utilized to investigate past and present-day terrestrial aqueous environmental conditions, and have recently been used in a GRS-based investigation of Mars (Taylor et al., 2006a, b; Karuntillake et al., 2006); this work largely forms the basis for Hypothesis 2 listed below, which attempts to explain the distinct elemental signatures in the northern plains.

To investigate the reported aqueous conditions described above, including both the possible formation of oceans and lakes and the transferal of rock materials from the highlands to the lowlands, we have performed a comparative analysis among the GRS (also see Boynton et al., 2002, 2004, 2007; Taylor et al., 2006a, b; Karunatillake et al., 2006; Keller et al., 2006; Hahn et al., 2007; Newsom et al., 2007), geologic, and topographic information discussed in the following.

3. GRS-based distributions of K, Th, and Fe

The Gamma Subsystem (GS) is part of a suite of instruments (Boynton et al., 2004) designed to detect a wide range of gamma-ray energies and energetic particles and neutrons emanating from the upper ~0.3 m near-surface materials of Mars and from cosmic rays. These instruments include the High Energy Neutron Detector (HEND), the Neutron Spectrometer (NS), and the GS; the three instruments of the GRS are designed to work synergistically to investigate the composition and nature of the near-surface Martian regolith (Boynton et al., 2004, 2007). Analysis of the data acquired from the GRS instrument suite has mapped the presence of significant subsurface ice deposits in regions poleward of approximately 60° north and south latitudes (Boynton et al., 2002; Feldman et al., 2002; Mitrofanov et al., 2002; Litvak et al., 2006), the distribution of H in low and mid latitudes (Feldman et al., 2004, 2005; Mitrofanov et al., 2004; Fialips et al., 2005), distinct elevated chlorine (Cl) regions (Keller et al., 2006), and other elements such as K, Th, Fe, and silicon (Si) (Boynton et al., 2007). These six elements of the Martian surface mapped through GRS have also formed the basis for evaluating the variations in K/Th (Taylor et al., 2006a), bulk composition (Taylor et al., 2006b), composition of northern low-albedo regions (Karunatillake et al., 2006), elemental abundances with respect to relative surface age (Hahn et al., 2007), geochemistry of Martian soil and bedrock in mantled and less mantled terrains (Newsom et al., 2007), and whether a giant ancient basin exists in Arabia Terra (Dohm et al., 2007a). In places, depletion of Si (Boynton et al., 2007) might well relate to Fe accumulation in ancient surface weathering environments (e.g., Noachian surface exposures).

Here, we take a close look at K, Th, and Fe in the equatorial and lower mid-latitude region of Mars roughly excluding the areas poleward of $\pm$50–60° latitude, where seasonal frost disturbs the measured abundances (also see Boynton et al., 2007). The GRS-based maps of K, Th, and Fe (Fig. 5) exhibit elevated concentrations in the reworked materials in and along the northern plains. Regions with greater than average K and Th include highly modified Noachian/Hesperian outcrops that both occur in patches in the northern plains such as Acidalia and Tartarus Colles and the regionally extensive Amazonian Vastitas Borealis Formation, all of which have been interpreted to be the result of sedimentary deposition (Tanaka et al., 2005), not withstanding that an ice mantle comprised of fine-grained materials may overlie parts of them (Soare et al., 2007). Another broad lowland region where K and Th are elevated is located to the northeast, southwest, and northwest of the northwest flank of Elysium rise where flows were emplaced into Utopia basin during the Early Amazonian Period. The flow materials, which have been mapped as the Tinjar a unit (unit Aet_a) and Tinjar b unit (unit Aet_b), are interpreted to be fluvial deposits, debris flows, and possibly lahars (Tanaka et al., 2005).

K and Th are also elevated in distinct parts of the cratered southern highlands, such as part of the ancient southern highlands province (including Terra Cimmeria and western part of Terra Sirenum; see Dohm et al. (2005), Taylor et al. (2006a, b), Karunatillake et al. (2007)). This geologic province displays both highly degraded macrostructures (tectonic features tens to thousands of kilometers long; Dohm et al. (2002)) and promontories (interpreted to be silica-enriched constructs such as andesitic domes; e.g., Hodges and Moore (1994)), among distinct

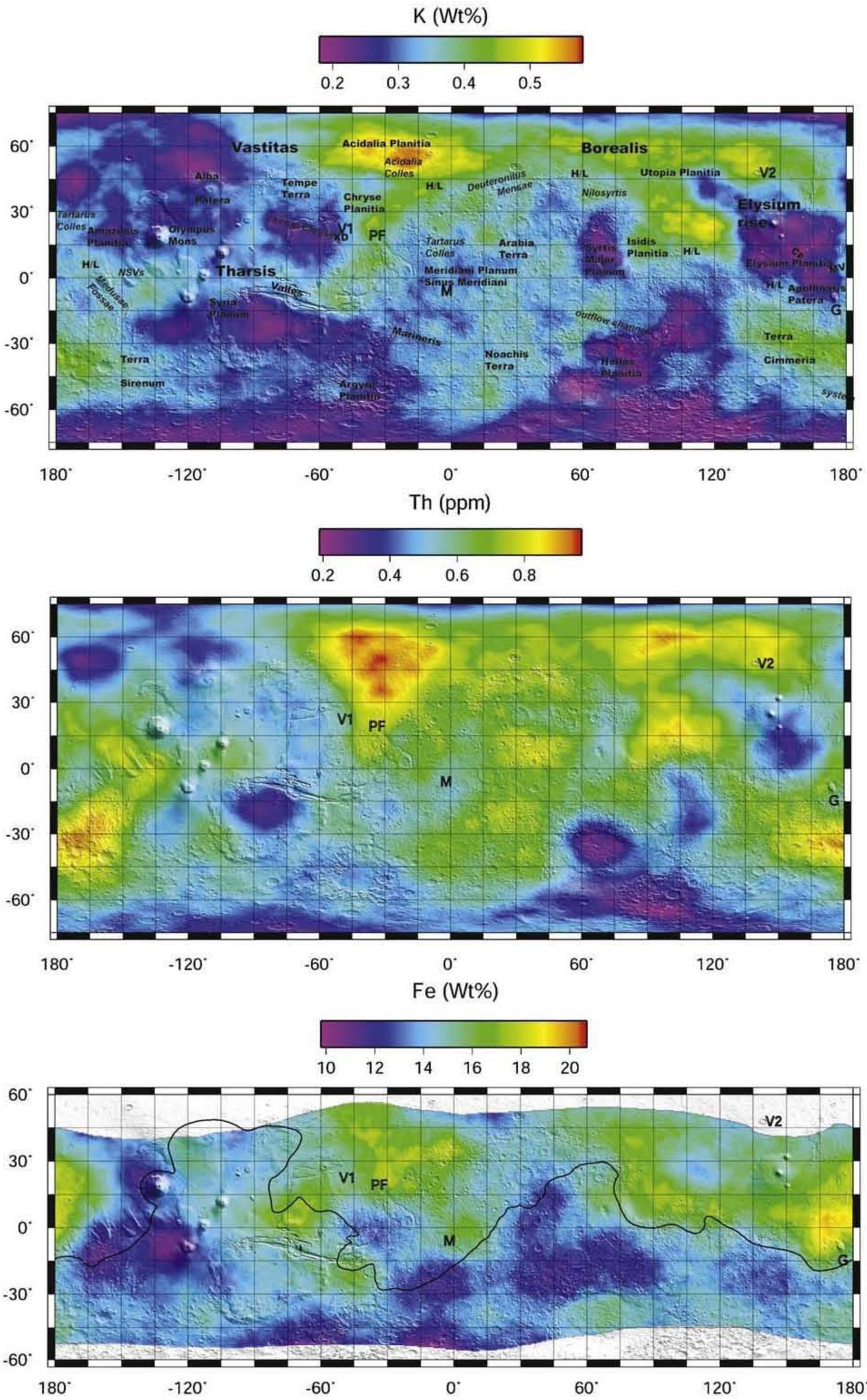

Fig. 5. GRS-based elemental map information showing K (top), Th (middle), and Fe (bottom) abundances (also see Boynton et al., 2002, 2004, 2007). Note that the elevated K and Th abundances in the northern plains include the Vastitas Borealis Formation hypothesized to have been emplaced by aqueous processes (e.g., Tanaka et al., 2005). On the other hand, K and Th abundances are low where Tharsis and Elysium volcanics have been mapped (e.g., Tanaka et al., 2003, 2005). Though Fe is visually elevated on the map, it is not statistically elevated in the northern plains when compared to the rest of the sampled region (also see Table 3). All nomenclature noted in the manuscript is shown at top, which includes Gusev crater (G), highland–lowland boundary (H/L), Xanthe Dorsa (XD), Marte Vallis (MV), Cerberus Fossae (CF), and general locations of MER Opportunity (M), Pathfinder (PF), and Viking 1 (V1) and 2 (V2).

magnetic signatures (Acuña et al., 1999, 2001; Arkani-Hamed, 2003, 2004; Connerney et al., 1999, 2005). These have been interpreted by some authors to mark a pre-Late Noachian era of plate tectonism (e.g., Baker et al., 2002, 2007; Dohm et al., 2002, 2005; Fairén et al., 2002; Fairén and Dohm, 2004; Connerney et al., 2005). A collection of such features occur on Earth where crustal accretion resulting from plate tectonism is recorded such as where oceanic plateaus have been slammed together, forming strong remnant banded magnetic signatures and macrostructures. These macrostructures occur along the margins or on trend with the banded magnetic signatures such as in Alaska (e.g., Fairén et al., 2002). Slightly elevated K and Th occur in the Arabia Terra

and Noachis Terra regions. The former has been reported to be a giant ancient basin (Dohm et al., 2007a) and the latter is a geologic province that straddles both the Argyre and Hellas impact basins, and thus includes ejecta deposits from both large impacts (Scott and Tanaka, 1986; Greeley and Guest, 1987).

In addition to the discernable regions of elevated K and Th concentrations, regions of low elemental concentrations are distinctly evident on the GRS maps (Fig. 5). Whereas the regions of elevated K and Th concentrations generally correspond with part of the ancient southern highlands province (Dohm et al., 2005; Karunatillake et al., 2007) and reworked rock materials in and along the margins of the northern plains, the low-concentration regions generally correspond with volcanic materials, as observed on published geologic maps (e.g., Tanaka et al., 2005). These include materials that contributed to the formation of the Tharsis, Elysium, and Syrtis volcanic provinces, particularly evident when viewed with the GRS K map draped over MOLA topography (Fig. 6). More specific examples include the Late Hesperian/Early Amazonian flow materials that emanate from Elysium rise and extend from the northwest flank into Utopia Planitia, as well as lava flows mapped on the western and eastern flanks of Elysium rise, the western and northern margins of Olympus Mons and Alba Patera, and the southeast flank of the complex shield volcano, Syria Planum (Scott and Tanaka, 1986; Greeley and Guest, 1987; Dohm et al., 2001a, c; Anderson et al., 2004; Tanaka et al., 2005).

Variations in Fe abundances are less pronounced on the GRS-based elemental maps when compared to K and Th in the northern plains, though elevated regions appear to generally include the eastern part of Chryse Planitia, Xanthe Dorsa, and the region that extends north into Acidalia Planitia. Another broad region of increased iron content includes Apollinaris Patera, extending north and northwest into the region east of Amazonis Planitia (including Tartarus Colles and Marte Vallis) and Elysium Planitia, respectively. This region is also elevated in both Cl and Th (Keller et al., 2006; Taylor et al., 2006a, b). Scott et al. (1995) identified Elysium Planitia as a possible paleolake basin and Marte Vallis as a spillway between the possible Elysium and Amazonis paleolakes (Fig. 7). These were later partly inundated by lavas (Plescia, 1990). Note that other possible paleolake locations such as Isidis, Chryse, and Utopia identified in the Scott et al. (1995) investigation also show elemental distinctions.

A distinctly low concentration of Fe is apparent along the western margin of the Tharsis magmatic complex, which includes the northwestern to western flanks of Olympus and Arsia Montes, as well as the Northwestern Slope Valleys (NSVs) region (Dohm et al., 2001a, b, 2004). Fe is also mostly low in the ancient cratered southern highlands when compared to parts of the northern plains.

It is evident that Fe, K, Th, and topography are not strictly correlated or anticorrelated (Figs. 5 and 6), though areas have anomalous high or low values of all three elements (e.g., Karunatillake et al., 2006, 2007; Taylor et al., 2006a, b; Boynton et al., 2007). Globally, a positive and almost linear correlation in the abundances of K and Th is observed (Karunatillake et al., 2006), consistent with primarily igneous fractionations since both

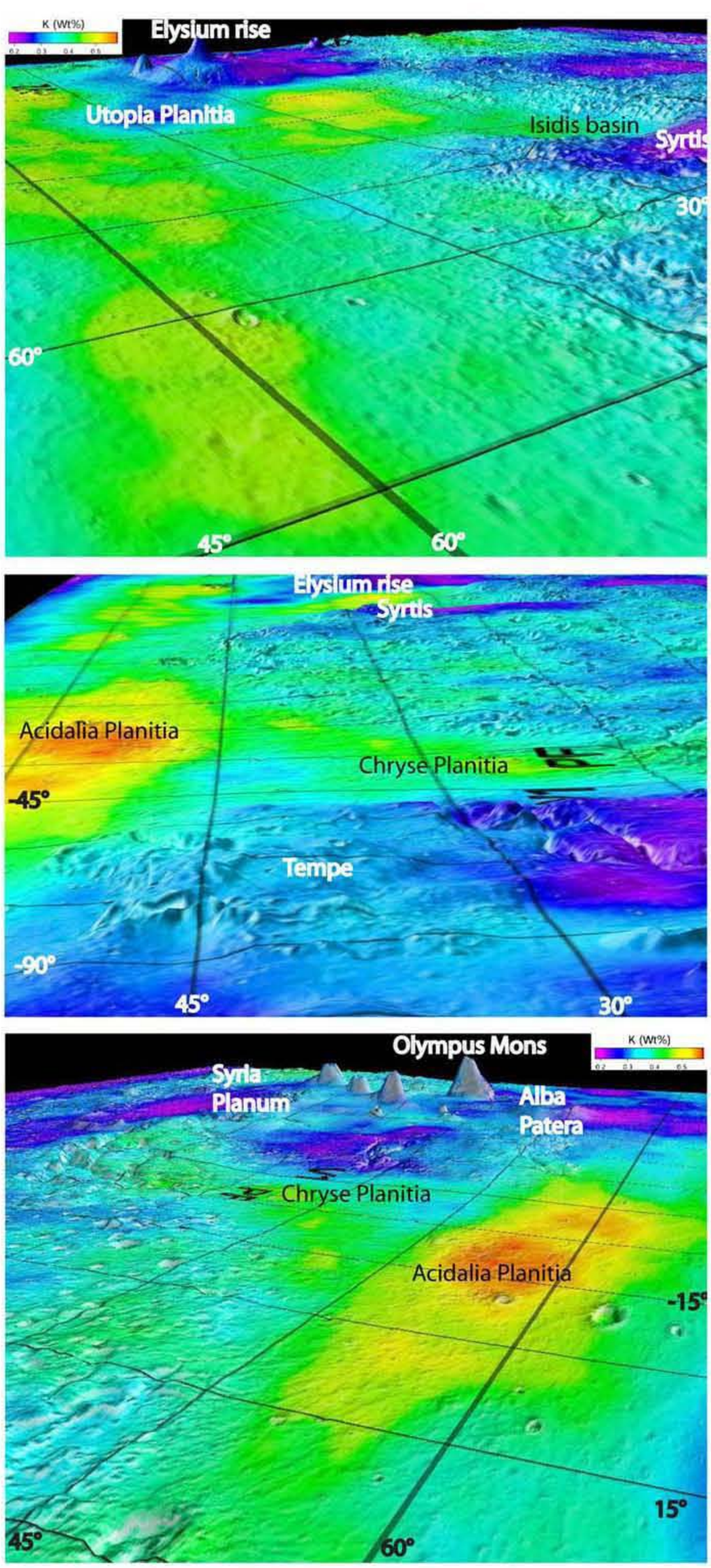

Fig. 6. 3D perspective images show the PDS released colorized GRS K concentration map over MOLA topography, including (top) an extreme 25X exaggeration looking obliquely to the southeast across the highland–lowland boundary towards the Utopia Planitia basin and Elysium rise (background), (middle) an extreme 30X exaggeration looking obliquely to the east–southeast along the highland–lowland boundary and across Tempe Terra plateau (foreground), Chryse Planitia, Acidalia Planitia, Syrtis, and Elysium rise (background), and (bottom) an extreme 25X exaggeration looking obliquely to the southwest along the highland–lowland boundary and across Acidalia Planitia, Chryse Planitia, and Tharsis rise, which includes giant shield volcanoes, Alba Patera, Syria Planum, and Olympus Mons (background). In all the perspectives, volcanic provinces clearly indicate low concentrations of K (violet to blue; see Fig. 5 for color-coded concentration scale), including the Elysium rise and associated flows that are emplaced into the Utopia Planitia basin (mapped as the Tinjar a unit (unit Aet_a) and Tinjar b unit (unit Aet_b) and interpreted to be fluvial deposits, debris flows, and possibly lahars by Tanaka et al. (2005)), Syrtis, and the Tharsis rise, which is comprised of giant shield volcanoes such as Syria Planum, Alba Patera, and Olympus Mons and large igneous plateaus such as Tempe Terra. Conversely, the degraded and deformed Noachian–-Hesperian materials along the highland–lowland boundary (dominantly the Nepenthes unit, unit HN_n, mapped by Tanaka et al. (2005)) and the regionally extensive Amazonian massive deposit that partly infills the northern plains, referred to as the Vastitas Borealis Formation (mapped, in part, as the Vastitas interior unit, unit ABv1, and interpreted to be sediments from Late Hesperian outflow channels among other processes by Tanaka et al. (2005)), are distinctly elevated in potassium (red to yellow; see Fig. 5 for color-coded concentration scale).

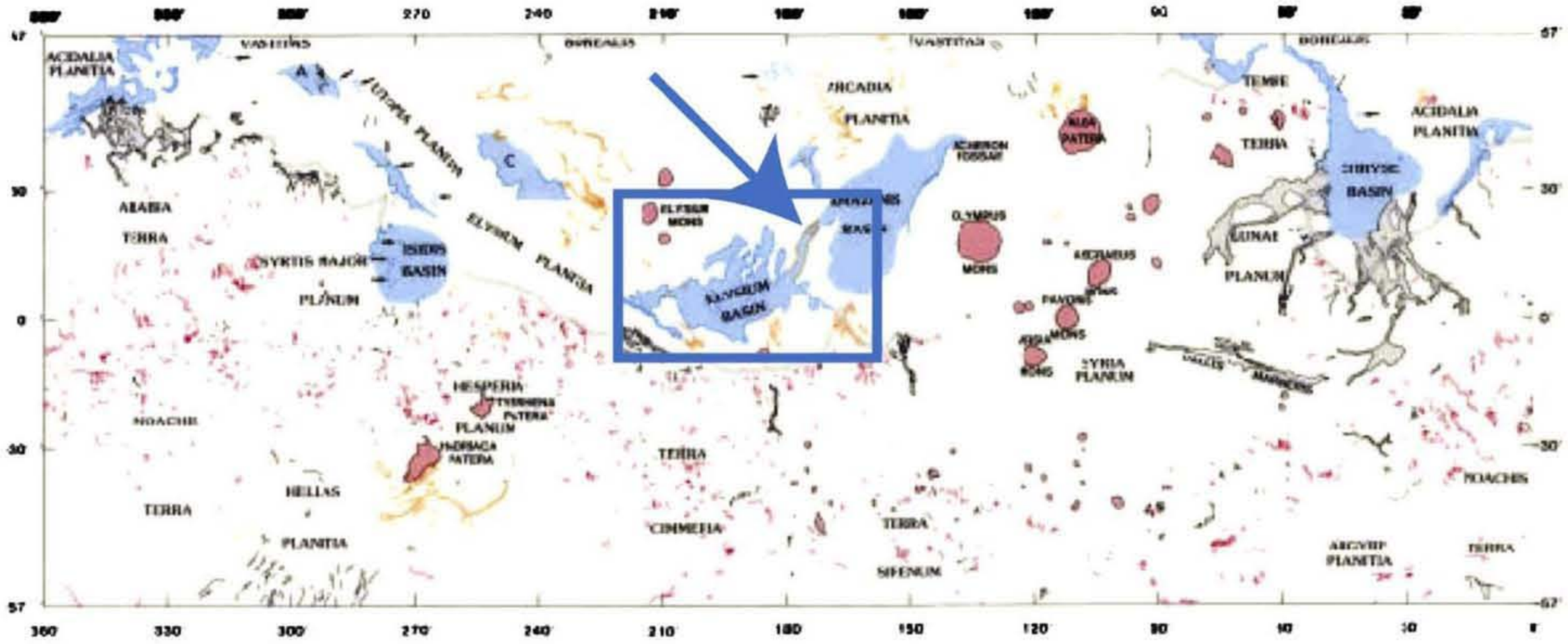

Fig. 7. Viking-based possible paleolake and channel map of Scott et al. (1995) through geologic, geomorphic, and topographic assessment; the highlighted blue regions mark possible paleolakes based on a list of geomorphic criteria while the lines indicate channels of varying relative age of formation (red Noachian, black Hesperian, orange Amazonian); also shown are volcanic constructs (red circular to irregular patterns), which includes Tharsis and Elysium, and a possible ancient spillway connecting the possible Elysium and Amazonis paleolakes (enlargement arrow and blue outlined region). Note that the possible paleolakes such as Chryse, Utopia, and Isidis record distinct elemental signatures (e.g., compare with the elemental maps of Fig. 5). Please see color version online.

K and Th are lithophile/mantle-incompatible elements; hence, K/Th ratios should exhibit much less variation than the elements by themselves as well. This is observed in general (e.g., Taylor et al., 2006a, b). However, there are some remarkable, rare departures where rather extreme fractionations of K and Th occur; these could be most readily attributed to aqueous fractionations, since K tends to be easily mobilized by water but Th is more resistant to solution processes; Hellas holds the most striking positive K/Th anomalies on Mars (Taylor et al., 2006a, b). On the other hand, there are lower than average K/Th anomalies that coincide spatially with the debouchment regions of the northeastern and northwestern watersheds of Tharsis, the circum-Chryse (e.g., Scott and Tanaka, 1986) and the Northwestern Valleys region (Dohm et al., 2001a, b, 2004), respectively. In the debouchment region of the circum-Chryse outflow-channel system, which includes Chryse and Acidalia Planitae, both distinct negative gravity anomalies and a continuation of outflow channels (into Acidalia) occur. This includes possible buried outflow channels (Fig. 2). Iron is less well correlated with K than K is with Th. In places it appears K and Fe are linked in their abundances, but elsewhere they seem nearly anticorrelated. Globally however, a significant correlation/anticorrelation between K and Fe is absent (Karunatillake et al., 2006).

4. GRS test for paleooceans on Mars

As a test of consistency of GRS data with the reported hypotheses for paleooceans on Mars, we compare the GRS, geologic, geomorphic, and topographic data to investigate the reported past aqueous conditions. This includes both the possible formation of oceans and lakes as well as the transferal of volatiles and rock materials from the highlands to the lowlands (e.g., see Baker et al., 1991; Scott et al., 1995; Clifford and Parker, 2001; Fairén et al., 2003, 2004; Tanaka et al., 2003, 2005). In order to perform the analysis, the following steps were taken. We first used reported paleoocean-boundary information (putative contacts/shorelines 1 and 2 based on, for example, Parker et al. (1987, 1993), Clifford and Parker (2001); Ruiz et al. (2003), and Fairén et al. (2003); the former reportedly marks at lease one great Noachian northern plains ocean, and the latter a Late Hesperian sea inset within the margin of the high water mark of the great ocean (Fairén et al., 2003), referred to as the older boundary and the younger boundary, respectively) and MOLA determined topography to derive regions for comparative analysis (Fig. 8). We then summed all the gamma-ray data acquired while the regions were frost free and the GS detector was head to the average elemental concentrations for the regions (Boynton et al., 2007). Finally, we investigated the spatial and temporal variations among common elements (Figs. 9–11). We use pairwise differences of mean concentrations (Tables 1–3) to determine whether apparent variations are statistically significant. The test parameter, t, is written as

$$t = \frac{\bar{w}_A - \bar{w}_B}{\sqrt{SE_A^2 + SE_B^2}} \quad (1)$$

where $\bar{w}_A$ is the mean mass fraction in region A, $\bar{w}_B$ is the mean mass fraction in region B, SE_A is the standard error of $\bar{w}_A$, and SE_B is the standard error of $\bar{w}_B$. This approach evaluates the Standard Normal distribution one-tail probability using t as the observed value and, importantly, it tests the distinctness of the means and not of the underlying distributions (Press et al., 2002; Karunatillake, 2008—in preparation). The test is less reliable with increasing disparity between SE_A and SE_B.

GRS-based comparative analysis reveals several distinctions among the regions. Both K (Fig. 9) and Th (Fig. 10) are clearly elevated in the regions that occur below the older and younger paleoocean boundaries with respect to the entire region (comparisons are made with the entire mid-latitudinal section of Mars, identified as the entire region; for more information see Boynton et al. (2007)); the younger boundary seems to be the more striking boundary with respect to separating areas of low K (above the boundary) to high K (below it). This observation is supported by the rejection of the null hypothesis, at 99% statistical confidence, that the regional mean K and Th contents are identical to the mid-latitudinal, entire-region means (Tables 1 and 2).

Although Fe appears elevated on the GRS map in parts of the northern plains, such as Acidalia Planitia, its concentrations in the boundary-defined regions are similar to those of the entire region at a level of $1-\sigma$ uncertainty (Fig. 11). There is a correspondingly low confidence that the null hypothesis can be rejected for the regions that occur below the older (78%) and younger (76%) boundaries (Table 3). While K is low in the regions that occur above the older and younger boundaries with respect to the entire region (Fig. 9), supported by a 99% confidence that the null hypothesis can be rejected (Table 1), Th in these regions approximates the concentration of the entire region (Fig. 10 and corresponding Table 2).

Is it possible that some other topographic or geologic boundary better isolates areas of high and low K abundance? We cannot rigorously exclude this possibility. But by inspection, the elevation represented by the younger boundary especially seems to be most significant, with a few notable exceptions, which diminish but do not obscure the global pattern established by K. These exceptions occur in areas where relatively young lavas of Tharsis and Elysium seem to have overprinted the younger boundary. Thus, a reasonable next step of our analysis was to remove the volcanic provinces based on Scott et al. (1986–87) from the regions shown in Fig. 8 (Fig. 12) and generate new elemental concentrations for statistical comparative analysis among the regions that include the volcanic provinces vs. the regions with the provinces removed (Tables 1–3). Following this step, there is a notable increase in the K values, but not for Th and Fe, such that the ranges of K t-test values decrease by a factor of two when comparing the region above the younger boundary vs. the region below the younger boundary and the region above the older boundary vs. the region below the older boundary. This is consistent with the observation that volcanic materials appear to be burying older K-rich rocks as noted above.

In summary, comparative analysis among GRS, geologic, geomorphic, and topographic information indicates that K and Th are elevated in the regions that occur below the older and younger boundaries when compared to the entire region. Thorium and especially K/Th ratios may be rich with insight (Taylor et al., 2006a), but the large errors on Th reduce its utility compared to K. The visually apparent increase in Fe concentration in parts of the northern lowlands when compared to the southern cratered highlands is *not* statistically significant when evaluated using the boundary-based regional information. However, visual inspection shows a strong and nonrandom pattern; consideration of variable H_2O abundances disallow that dilution effects are controlling the pattern. The fact that for Fe (Fig. 11) there is substantially less variability in the boundary-delineated regions than can be assessed by eye from the map says that, unlike the case for K, the boundaries are not the prime demarcations or the only demarcations isolating Fe-rich and Fe-poor regions. Some of these apparent Fe-rich regions overlap with K- and Th-rich regions, but there is neither a visible one-to-one correspondence nor a correlation in multivariate space (Karunatillake et al., 2006). Hence, K and Fe appear to vary independently across Mars. This is

the proximal locations (Fig. 2). Distinct lower than average K/Th anomalies (Taylor et al., 2006a, b), which coincide spatially with the debouchment regions of the northeastern and northwestern watersheds of Tharsis, the circum-Chryse (e.g., Scott and Tanaka, 1986) and the NSVs region (Dohm et al., 2001a, b, 2004), respectively, is consistent with this scenario, as both K and Th may result from leaching of highland materials. They are concentrated at the major break in slope of the highland–lowland boundary, where Th would concentrate at the break in slope when compared to the more mobile Fe. Iron, on the other hand, appears concentrated at levels above the global mean throughout the region of Acidalia Planitia and Vastitas Borealis, though its concentration is also low in the NSVs region, the eastern part of the circum-Chryse outflow channels, and along the floor of the highly degraded Chryse impact crater, where central and western parts of the outflow system debouch. K and Fe, therefore are not strictly linked, although the seeming elevated abundances in Fe in the basin suggests either solution transport and deposition or concentration due to clastic grain winnowing; hematite, ilmenite, magnetite, and some other iron minerals may have the hardness and durability to survive long distance transport as bed load or suspended load. However, we must allow that solution transport in acidic brines may have leached Fe from the highlands and deposited it in the basin, realizing that Fe solubility starts at about pH 4.0, rising slowly to pH 3.0 and increasing logarithimically towards pH 2.0, and that sufficiently large concentrations of H^+ need to be present to render Fe soluble (Birkeland, 1999). Unless affected by acid rain or mining spoil (e.g., Wai et al., 1980) such as reported for the Tinto River in Spain (Fernández-Remolar et al., 2004), soils on Earth generally have pH's above 4.0 and Fe is insoluble unless organically complexed. On Mars, acidic aqueous environmental conditions prevailed for at least part of its history and at least of local to regional extent, as evidenced from the jarosite-containing sedimentary outcrops of Meridiani Planum (Fairén et al., 2004; Squyres et al., 2004).

Distinct magma sources may also explain elemental enrichment in parts of the northern plains (Karunatillake et al., 2006), as detailed below in Hypothesis 2. Importantly, the distinct elemental signatures in the northern plains may mark both a diversity in rock compositions (e.g., rocks of the ancient southern highlands province, including distinct parent magma bodies vs. younger Tharsis/Elysium, etc., volcanics) and environmental, geological, and paleohydrological conditions, which include possible oceans and their associated variety of depositional and erosional mechanisms. In addition, the lower than average K/Th anomalies in the debouchment regions of the northeastern and northwestern watersheds of Tharsis could reflect inherent K/Th of the Amazonian lava flow materials from Tharsis (Taylor et al., 2006a, b).

With the exception of the ancient southern highland province and the Arabia Terra province (Dohm et al., 2005, 2007a), pronounced elevated K and Th signatures of rock materials of the southern cratered highlands, which includes sedimentary sequences, may be obscured by younger Tharsis activity, as well as large impacts, which include post-magnetosphere Hellas, Argyre, and Isidis (Arkani-Hamed, 2004). The impact events would have harvested mantle materials when the environmental conditions were drastically different from a more ancient time. Pre-impact conditions, for example, would include an operating magnetosphere, elevated planetary heat flow (e.g., Schubert et al., 1992), a relatively thin lithosphere, and a competition among heavy bombardment and high erosion rates, including impacts occurring during the formation of fluvial and alluvial deposits (Malin and Edgett, 2000, 2001; Baker et al., 2007). Though Hellas, Argyre, and Isidis impact basins and surroundings record wind- and water-related weathering, as well as weathering in the form of precipitates on grain surfaces, volcanic resurfacing (e.g., Scott and Tanaka, 1986; Greeley and Guest, 1987; Crown et al., 1992; Leonard and Tanaka, 2001; Moore and Wilhelms, 2001), and impact-induced structures such as structurally controlled valleys and basins and faults concentric and radial about the central part of the basins, the primary impact basins themselves are still clearly prevalent (Dohm et al., 2002; Baker et al., 2007). On the other hand, older impact basins such as Utopia (e.g., Tanaka et al., 2005) and the hypothesized Arabia Terra (Dohm et al., 2007b) basins are all but destroyed to the untrained eye by burial and deformation, indicating environmental conditions drastically different from those at the time when the Hellas, Argyre, and Isidis events occurred. Following the shutdown of the magnetosphere, Tharsis, and to a lesser extent, Elysium, would dominate the geologic record for more than 3.5 Ga, which includes local to global distribution of volcanics by wind and water (Fairén and Dohm, 2004; Baker et al., 2007), though processes related to orbital parameters (e.g., glaciation; e.g., see Head et al. (2003)) and atmospheric conditions (persistent winds) would attempt to overprint geologic and paleohydrologic/weathering records.

5.2. *Hypothesis 2. Igneous processes and secondary alteration*

Based on a comparison among MGS-TES, Pathfinder, and Viking IRTM datasets, the elemental information may be explained by inherent variations in igneous rocks and by variations in the extent of aqueous alteration. For example, the TES-derived surface type 2 areal fractions, K mass fraction, and Th mass fraction are spatially correlated throughout Mars, with marked enrichment of all three in low-albedo regions of the northern lowlands (Karunatillake et al., 2006). As explained by Karunatillake et al. (2006) and Taylor et al. (2006a), this observation is consistent with a surface type 2 primary mineralogy derived from a magma source that is distinct from any that contributed to surface type 1 material in the southern highlands. Due to the globally strong spatial coupling of K and Th, secondary alteration (be it moderate pH or low pH) is less likely to have yielded the GRS elemental signature for surface type 2 (e.g., Karunatillake et al., 2006; Taylor et al., 2006a), except perhaps as surficial micrometer-thick rinds detectable at MGS-TES sampling depths (Rogers and Christensen, 2007). Nevertheless, detectable variations in the K/Th ratio of meaningful spatial extent occur in a few localities, suggesting some degree of aqueous alteration (Taylor et al., 2006a).

5.3. *Earth analogues*

Based on terrestrial investigations, minerals that comprise K and Th provide important clues to the formational conditions and mechanisms (e.g., accumulations) that may have resulted in the GRS-based elemental signatures identified for the regions of special interest shown in Fig. 8. For example, some fraction of K may be locked in salt minerals such as sylvite (KCl) and carnallite ($KMgCl_3 \cdot 6H_2O$) in the northern plains. These K salts on Earth commonly form in playa (dry lake) environments that may have wet episodes during which water inundates the whole area (Ori et al., 2001; Komatsu et al., 2007). The formation of evaporite deposits includes the reworking of parent rock materials (e.g., leaching) and transport and subsequent precipitation; this process can be enhanced during acidic aqueous conditions as is commonly associated with mining operations (e.g., Taylor et al., 2006a). One of the best examples of the influence of mining on environmental conditions, which includes acidic aqueous conditions, leaching, transport of rock materials including elements, and precipitation of minerals such as hematite and jarosite, is the Tinto River in Spain (Fernández-Remolar et al., 2004).

Table 2
Similar to Table 1, but investigation of the spatial and temporal variation of Th among the paleoocean boundary-defined regions including and excluding the volcanic provinces (also see Figs. 8, 10 and 12)

Region	Times	*t*-Parameter (regions with volcanic provinces)	*t*-Parameter (regions without volcanic provinces)	Probability (refer Eq. (1) and related text for description). Probability with:without volcanic provinces
Entire	41932000	0.00	0.00	50%:50%
Below younger	6582100	3.27	2.58	0%:0%
Above younger	35320000	0.60	0.85	28%:/20%
Below older	16028000	2.18	1.75	1%:4%
Above older	25835000	0.33	0.74	37%:23%

Table 3
Similar to Table 1, but investigation of the spatial and temporal variation of Fe among the paleoocean boundary-defined regions including and excluding the volcanic provinces (also see Figs. 8, 11 and 12)

Region	Times	*t*-Parameter (regions with volcanic provinces)	*t*-Parameter (regions without volcanic provinces)	Probability (refer Eq. (1) and related text for description) Probability with:without volcanic provinces
Entire	41932000	0.00	0.00	50%:50%
Below younger	6582100	0.71	0.73	24%:23%
Above younger	35320000	−0.26	−0.17	40%:/43%
Below older	16028000	0.79	0.90	22%:18%
Above older	25835000	−0.37	−0.73	36%:23%

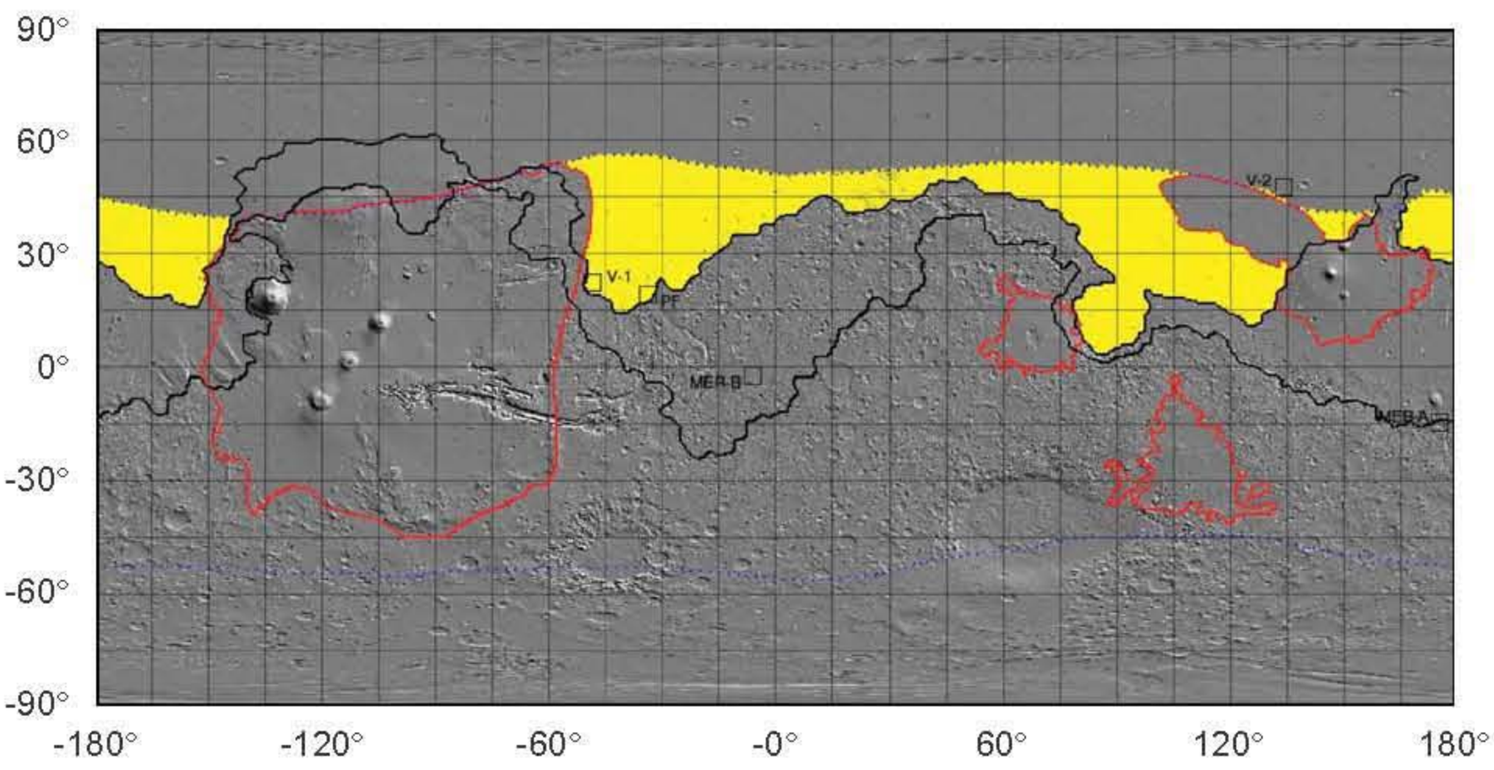

Fig. 12. Volcanic provinces (red outlined regions) were removed from the shoreline-defined regions (e.g., Fig. 8) such as in the case of the region that occurs below the younger paleoocean boundary for generating new elemental concentrations and comparing the associated statistical information with the information corresponding to the regions that included the provinces (Tables 1–3). Please see color version online.

volcano (e.g., Keller et al., 2006; Taylor et al., 2006a, b; Dohm et al., 2008)). Sedimentary records could also be subdued by mantles of ice and fine-grained materials (Murray et al., 2005; Soare et al., 2007) and/or aeolian deposits. The highland–lowland boundary has been degraded and deformed, exposing the ancient (e.g., Noachian) stratigraphic records (including possible flood, marine, and lacustrine deposits, which may have been locally derived and/or include materials from regional highland provenances). The vast region marked by the Vastitas Borealis Formation, possibly marking a MEGAOUTFLO event, may be older crustal materials similar to those of the southern ancient province harvested from flooding and deposited in the northern plains to form a laterally extensive deposit (e.g., source materials include volcanic materials of the eastern Tharsis basin; e.g., Dohm et al. (2001a)).

K can be concentrated in feldspathic sands by winnowing of clastic mineral grains, or it can be strongly fractionated via dissolution and precipitation in aqueous media. Th is much more resistant to dissolution, but it will dissolve in acidic solutions. A more common means of fractionation, however, is by winnowing of monazite, zircon, and other Th-rich mineral grains; this is common in saltation processes due to the high densities of these minerals relative to many other hard sand-forming minerals.

One scenario is that Th-rich mineral sands were deposited preferentially in the flood-debouchment parts of the basins near the highland–lowland boundary, whereas K tended to be dissolved and precipitated farther into the basin over time. This situation is consistent with northward migration of K in outflow channels waters and basinal fluids and final preferential deposition of K in the more distal zones, with Th concentrated more in

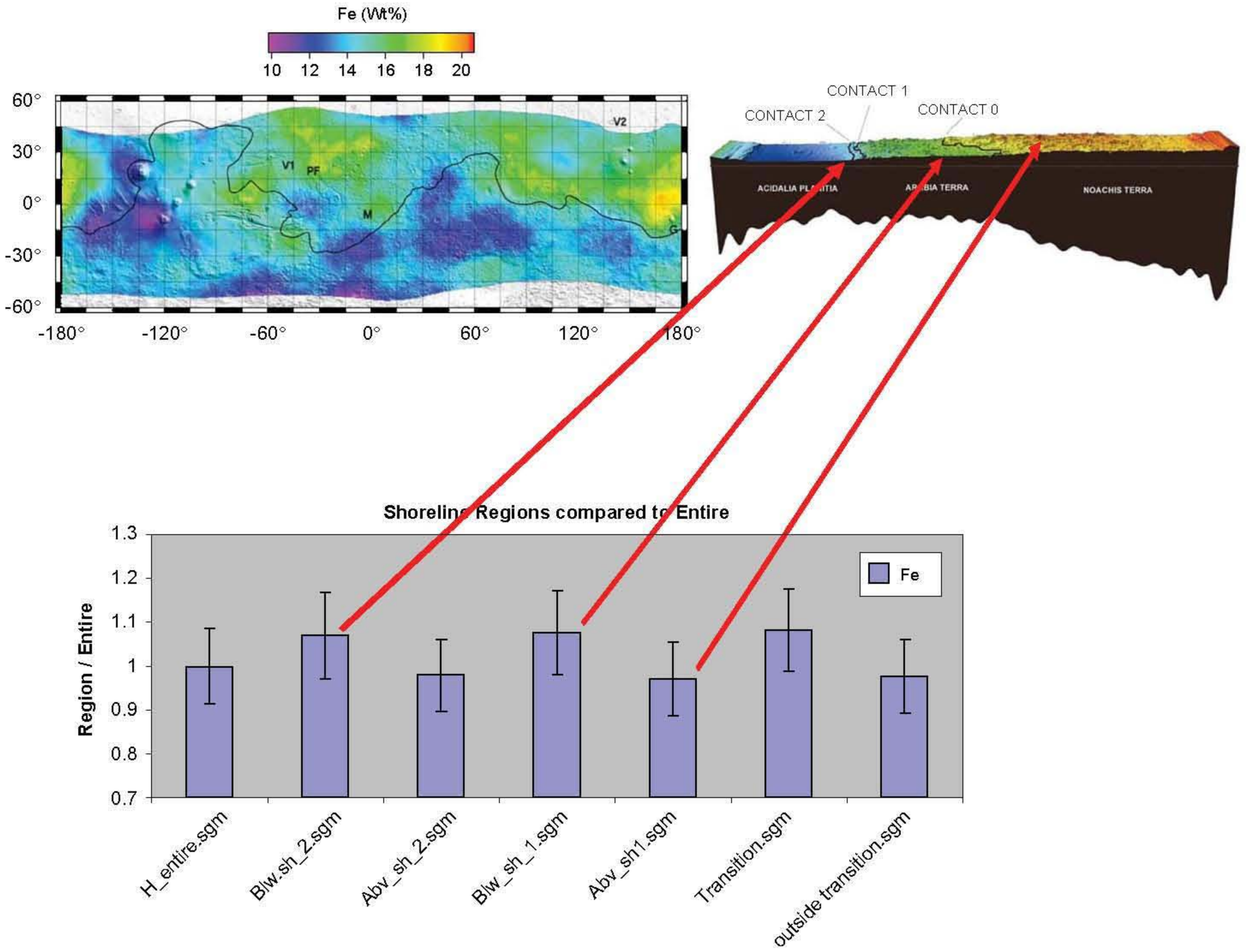

Fig. 11. Similar to Figs. 9 and 10, but spatial and temporal Fe information among the regions, including ratios of regional mean compositions to that of the entire mid-latitudinal section of Mars (noted below as the entire region; for more information see Boynton et al., 2007). Statistical significance of the difference is presented in Table 3. GRS-based comparative analysis reveal that although Fe appears elevated on the GRS map in parts of the northern plains, its concentration in the various regions is similar when compared to the entire region, and there is relatively little confidence that the null hypothesis can be rejected for the regions that occur below the older and younger paleoocean boundaries (only at 78% and 76% confidences, respectively; Table 3).

Table 1
Investigation of the spatial and temporal variation of K among the paleoocean boundary-defined regions including and excluding the volcanic provinces (also see Figs. 8, 9 and 12 for region definition), using pairwise differences of mean concentrations to determine whether apparent variations are statistically significant

Paleolake boundary region	Times	*t*-Parameter (regions with volcanic provinces)	*t*-Parameter (regions without volcanic provinces)	Probability (refer to Eq. (1) and related text for description). Probability with:without volcanic provinces
Entire	41932000	0.00	0.00	50%:50%
Below younger	6582100	16.32	17.71	0%:0%
Above younger	35320000	−4.07	6.58	0%:0%
Below older	16028000	9.08	13.7	0%:0%
Above older	25835000	−4.53	6.10	0%:0%

Information includes gamma-ray captures over time as the spacecraft passes a region (times), *t*-parameter values for the regions, and probability. We seek to determine whether the regional average is distinct from average Mars using the null hypothesis: the regional mean K content is identical to the mid-latitudinal "entire region" mean (for details, see Boynton et al., 2007). Importantly, this test evaluates the distinctness of the means, not of the underlying distributions.

Th-enriched sedimentary records marking past conditions are obscured in places to the GRS instrument by burial through the emplacement of volcanic materials (e.g., Tharsis and Elysium magmatic complexes and local fissure-fed eruptions that mostly mark relatively low elemental concentrations (Fig. 6), except for Cl and Fe that are elevated in mostly stratigraphically young parts of the Tharsis and Elysium magmatic complexes, the Medusae Fossae Formation, and the seemingly isolated Apollinaris shield

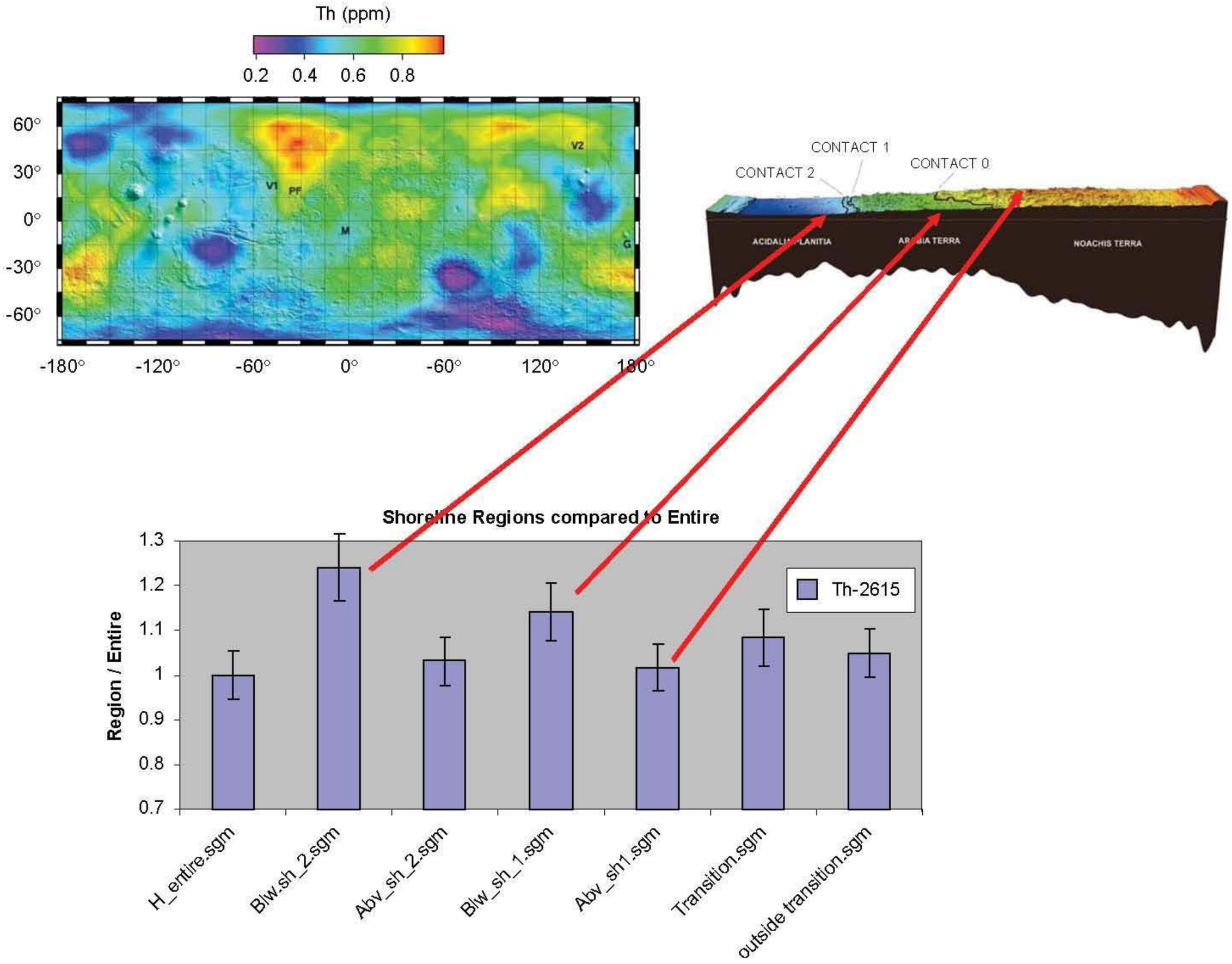

Fig. 10. Similar to Fig. 9, but spatial and temporal Th (A) information among regions, including ratios of regional mean compositions to that of the entire mid-latitudinal section of Mars (noted below as the entire region; for more information see Boynton et al., 2007). Statistical significance of the difference is presented in Table 2. GRS-based comparative analysis reveal distinctions among the regions, including that Th: (1) is clearly elevated in the regions that occur below the older and younger paleoocean boundaries with respect to the entire region, supported by the rejection of the null hypothesis at 99% statistical confidence: "the regional mean Th content is identical to the mid-latitudinal, entire-region mean" (Table 2), and (2) Th approximates the concentration of the entire region when compared to the regions that occur above the older and younger paleoocean boundaries.

wet surface weathering microenvironments subjected to high abrasion pH levels initially rendering Al soluble followed by crystallinity below pH 8.0 based on terrestrial investigations (e.g., Birkeland, 1999); and (6) Martian orbital parameters and related environmental/climatic changes (see Carr, 1990; Touma and Wisdom, 1993; Laskar and Robutel, 1993; Head et al., 2003) and persistent wind activity that partly overprint earlier major endogenic-driven activity. GRS records such reported changes in planetary conditions.

Below are hypotheses that attempt to explain the elemental signatures described above, including (1) resurfaced rock materials (e.g., materials exposed through highland–lowland degradation and deformation and hydrologic activity such as Tharsis-driven flooding and spring-fed activity), and (2) igneous processes and secondary aqueous alteration, as well as potential terrestrial analogue information.

5.1. Hypothesis 1. Resurfaced materials

Significantly, the distinctions of elemental concentrations in regions delineated by paleoocean boundaries are consistent with published geologic information (Dohm et al., 2007c). Elevated K and Th in the regions that occur below the older and younger boundaries when compared to the entire region is amply explained by reported geologic and paleohydrologic activity, which includes Tharsis-driven activity (and to a lesser extent, Elysium rise during the Hesperian/Amazonian). As reported above, this includes flooding, changing environmental and atmospheric conditions, spring-fed activity, leaching of paleosols in cratered highland materials, transport of rock materials and volatiles from the highlands to the lowlands, and ponding in the northern plains to form transient water bodies from lakes to oceans (Baker et al., 1991, 2002; Fairén et al., 2003). These K- and

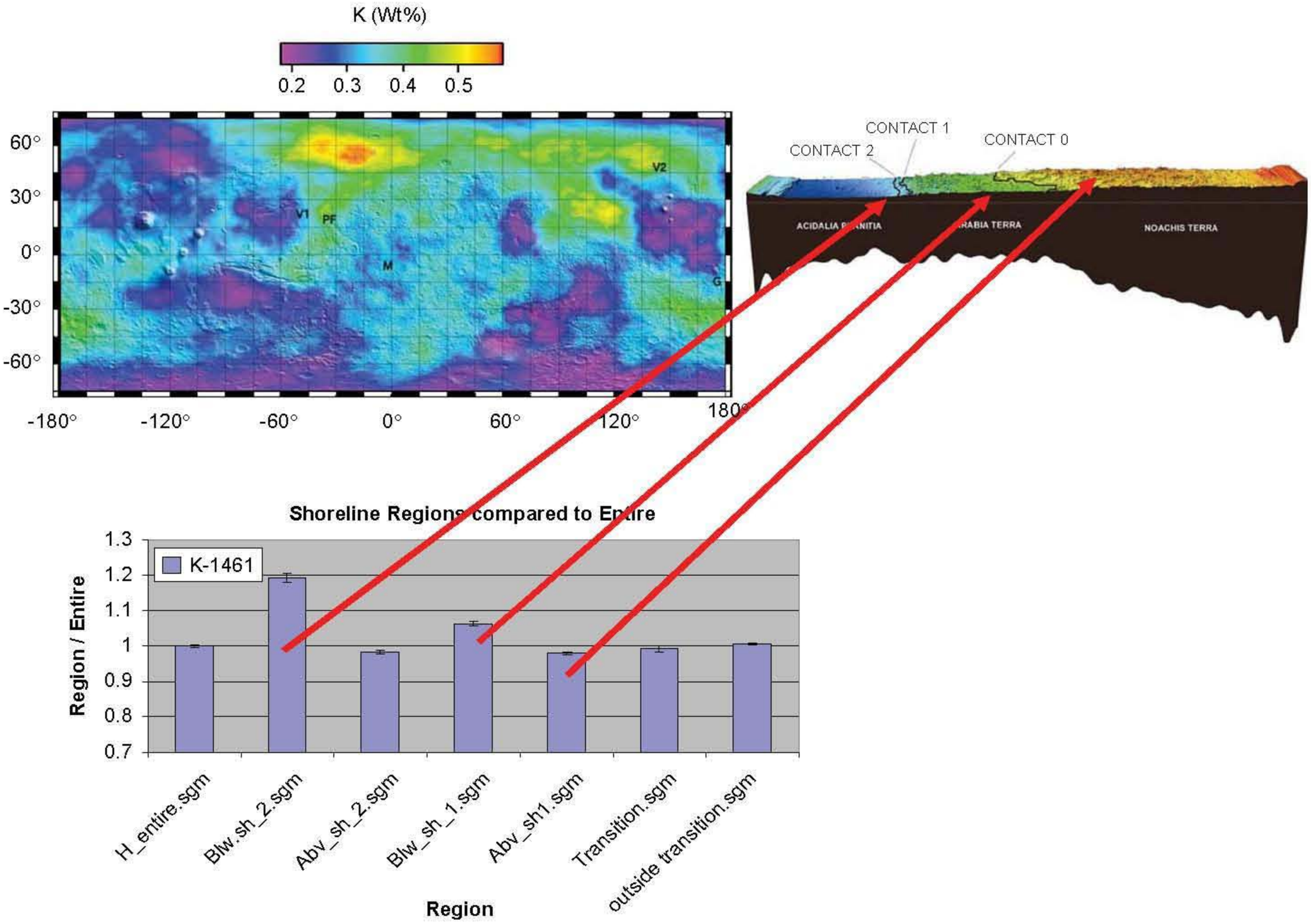

Fig. 9. Spatial and temporal K information among the paleoocean-boundary-defined regions (also see Fig. 8), including ratios of regional mean compositions to that of the entire mid-latitudinal section of Mars (noted below as the entire region; for more information see Boynton et al. (2002, 2004, 2007)), which includes a cross-sectional profile (based from Fairén et al. (2003); note that in this particular transect, labeled Contacts 1 and 2 approximate the younger paleoocean boundary and Contact 0 approximates the older paleoocean boundary) and histograms (bottom; note that label sh 2 represents the younger paleoocean boundary, sh 1 represents the older paleoocean boundary, and transition is the region between the younger and older boundaries) within 1-sigma error showing paleoocean-boundary regions compared to the entire region. The paleoocean-boundary demarcations are annotated on a cross section of inferred crustal thickness from MOLA data (image from MOLA Science Team), running from the north pole (left) to the south pole (right), along the 0° longitude region, including Arabia Terra. Statistical significance of the difference is presented in Table 1. GRS-based comparative analysis reveal distinctions among the regions, including that K is (1) elevated in the regions that occur below the older and younger paeloocean boundaries with respect to the entire region, supported by rejection of the null hypothesis at 99% statistical confidence: "the regional mean K and Th contents are identical to their respective mid-latitudinal, entire-region mean" (Table 1), and (2) low in the regions that occur above the older and younger paeloocean boundaries with respect to the entire region, supported by a 99% confidence that the null hypothesis can be rejected (Table 1).

in the Discussion eologic history of Mars is far from static through detailed geologic investigation, which takes into consideration diverse perspectives through detective work, including comparative analysis among the stratigraphic, paleotectonic, geomorphic, topographic, geophysical, spectroscopic, and particularly in this case, the GRS-based elemental information. This includes extreme variations in endogenic and exogenic conditions from ancient to present Mars (Baker et al., 2007), such as: (1) crustal/lithospheric and heat flow conditions (e.g., through time, crustal/lithospheric thickness increases, tectonism decreases but becomes concentrated near the large shield volcanoes, and heat flow diminishes, all of which have a significant effect on ancient vs. present-day topographies; e.g., Schubert et al. (1992), Scott and Dohm (1997), Dohm et al. (2001a), Anderson et al. (2001), McGovern et al. (2002, 2004), Fairén et al. (2003), Ruiz (2003), Ruiz et al. (2004)); (2) impact cratering (Neukum et al., 2001), especially with respect to the period of reported impact catastrophism (Strom et al., 2005); (3) surface and near-surface conditions (sratigraphic, tectonic, geomorphic, mineralogic, geochemical, geophysical, and topographic, etc.; e.g., see Scott and Tanaka (1986), Dohm et al. (2001c), Fairén et al. (2004), Fairén and Dohm (2004), Connerney et al. (2005), Tanaka et al. (2005), Taylor et al. (2006a, b), Karunatillake et al. (2006), Keller et al. (2006), Hahn et al. (2007), Newsom et al. (2007), Boynton et al. (2007)); (4) atmospheric and environmental conditions (e.g., Baker et al., 1991), such that aqueous conditions, which may have been less acidic to form clays early on in the weathering microenvironment, gave way to more acidic long-lasting conditions to form sulfates (Bibring et al., 2006) and/or acidic clay minerals such as kaolinite and halloysite, largely related to the growth of the dominant, yet enduring development of the Tharsis superplume pulsating from the Noachian to the Amazonian (Dohm et al. 2001a, 2007b) and to lesser magmatic complexes such as Elysium (e.g., Tanaka et al., 2005); these heat engines were episodically active to interrupt the long-persistent, cold–dry state for relatively short transient periods; (5) clay genesis of (4) would result from ancient

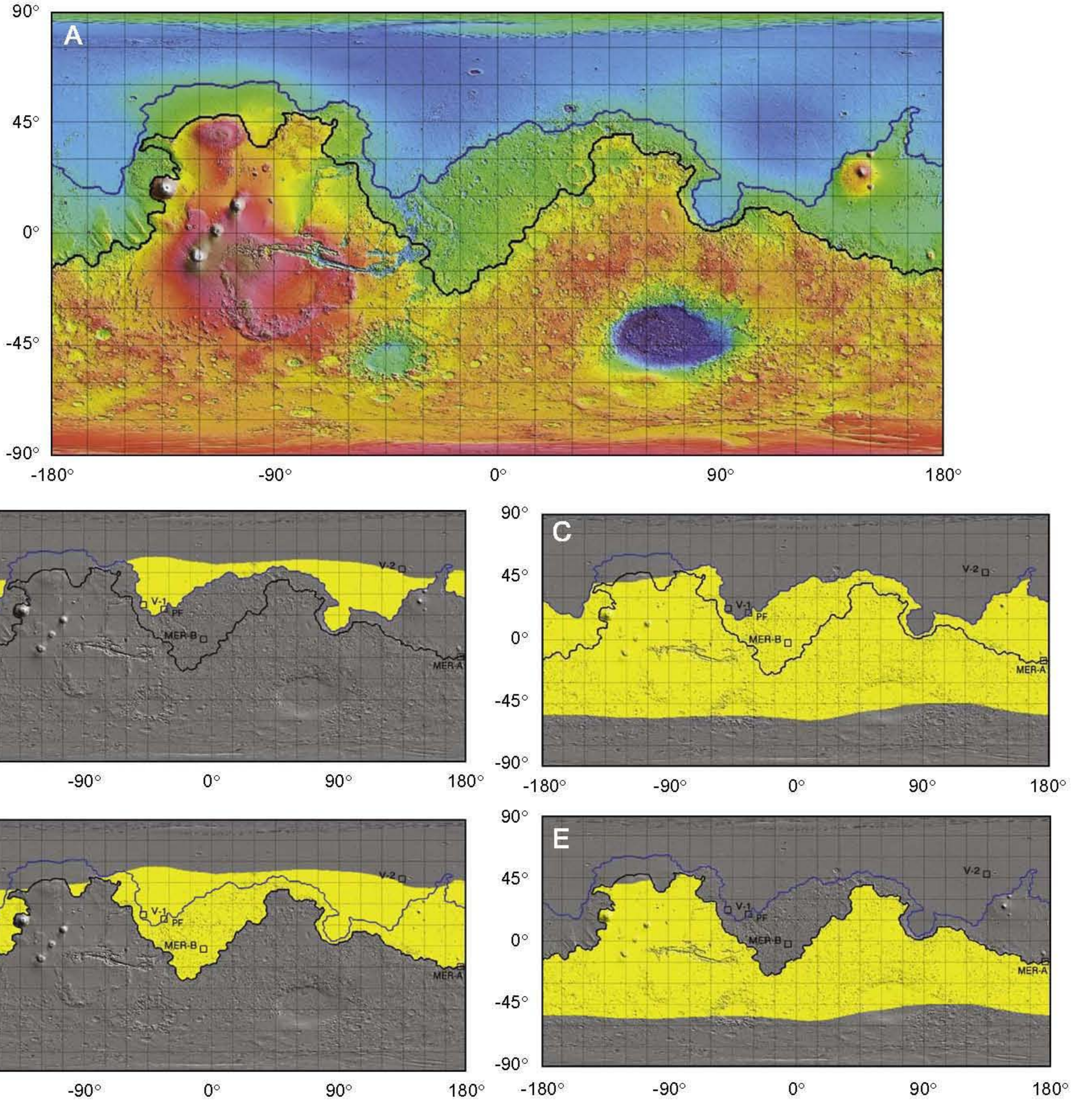

Fig. 8. Paleoocean-boundary information (including Parker et al., 1987, 1993; Clifford and Parker, 2001; Ruiz et al., 2003; Fairén et al., 2003) placed on MOLA data prepared for regional GRS summing (A). In addition, yellow regions on MOLA shaded relief maps denote: region below younger paleoocean boundary (B), region above younger paleoocean boundary (C), region below older paleoocean boundary (including younger boundary) and (D), region above older paleoocean boundary (E). Please see color version online.

a strong indication that variations in the distribution of one mineral or rock type do not control K and Fe abundances. Rather, it is more complex. In the Chryse Basin, both Fe and K tend to be visibly concentrated together, whereas in the Utopia Basin, K is concentrated but Fe is visibly less so.

Whereas K is low in the regions that occur above the older and younger boundaries, Th approximates the entire region. These distinctions are largely consistent with existing geologic information. For example, K and Th are elevated in parts of the ancient southern highlands province (Dohm et al., 2005; Taylor et al., 2006a, b; Karunatillake et al., 2007), and in regionally extensive outcrops of reworked materials in parts of the northern plains and along the highland–lowland boundary, interpreted to be sedimentary deposits (e.g., ancient materials that are the result of degradation/retreat of the highland–lowland boundary and more recent Vastitas Borealis Formation; see Tanaka et al. (2005)). On the other hand, low elemental concentrations of K, Th, and Fe correspond generally to regionally extensive volcanic deposits as noted above, such as observed for most of the Tharsis region and the flow materials that emanate from the Elysium rise and extend into the Utopia basin (Fig. 6). These distinctions unfolded through comparative analysis and the general consistency among existing GRS, geologic, geomorphic, and topographic information will be further discussed in the presentation of our working hypotheses

Meridiani Planum, which is part of the northern plains, was recently suggested to have been a playa based on Mars Exploration Rover results (Grotzinger et al., 2005) or a region that records the transgression and regression of acidic oceans (Fairén et al., 2003, 2004). Thus, enhancement of potassium in the upper $\frac{1}{3}$ m of the northern plains could be interpreted as an indication for the accumulation of salts that resulted from desiccation of potassium-rich water, and other elements such as Th enriched due to leaching highland materials, transport, and eventual concentration in the northern plains. Inconsistent with this hypothesis, however, the GRS-based elemental abundance of Cl is mostly moderate to low in the northern plains (Keller et al., 2006). Though, at resolution, GRS cannot map out expected localized variations in Cl due to its high solubility, as observed at Gusev and Meridiani through the MER rovers, Spirit and Opportunity, respectively (Squyres et al., 2004). There are GRS-based patterns of significantly elevated Cl. However, these spatially correspond to geologically youthful terrain such as the Medusae Fossae Formation and surrounding terrain attributed to denudation of volcanic ignimbrite deposits enriched in Cl through acid–fog reactions (at some point in the formation's history) and/or some other aqueous activity, including transport of Cl in liquid ground or surface water (Keller et al., 2006; Boynton et al., 2007; Dohm et al., 2008); hence, the lack of Cl signature in the northern plains may also reflect time and degree of modification of the rock materials. Importantly, materials from distinct parent magma bodies whether in situ and/or derived from regional provenances (Taylor et al., 2006a, b; Karunatillake et al., 2006) may also contribute to the GRS elemental signatures. In terrestrial playa environment, circulation of groundwater continues even after the wet episodes end. And the circulation of groundwater further contributes to accumulation and deposition of salts. It is conceivable, if not probable, that Martian groundwater circulation continued long after the wet episodes ceased, enhancing the accumulation of potassium salts. This view is consistent with diagenesis resulting in the formation of hematite-rich spherical balls that were interpreted to be concretions (Chan et al., 2004; Ormö et al., 2004b). If acidic conditions prevailed for long durations, then such diagenesis-related processes would be enhanced (Taylor et al., 2006a) and elements such as K and Th would be leached and transported from the highlands to concentrate in the lowlands.

Recent work has shown Fe to be significantly enriched in close proximity to the highland–lowland boundary, occasionally in association with other elements (e.g., Karunatillake et al., 2007). We find three regions of elevated Fe: (1) a region, which straddles the southeast margin of the Elysium rise and the northwest margin of Gusev Crater, which includes Elysium Planitia and Apollinaris Patera, (2) the highland–lowland boundary region located along the south–southwestern margin of Utopia Planitia, which includes Isidis Planitia, and (3) a region that includes the eastern–northeastern part of Chryse Planitia and south–central part of Acidalia Planitia (Karunatillake, 2008—chemically striking regions of Mars, in preparation). These are particularly interesting from the perspective of past aqueous activity because they have been identified as sites of long-lived magma–water interactions particularly in the case of Apollinaris Patera (Scott et al., 1995) and the Cerberus plains (Burr et al., 2002) and paleolakes particularly in the case of the above listed planitiae (Scott and Chapman, 2005; Scott et al., 1995). Activity may include periglacial and glacial resurfacing, including ice mantles enriched with fine-gained materials (Head and Pratt, 2001; Kargel, 2004; Head et al., 2006a, b; Kostama et al., 2006; Soare et al., 2007) that could subdue the GRS signatures. Significantly, the Fe-enriched planitiae regions correspond with rock materials, which have been mapped, characterized, and interpreted to include sedimentary origin (Tanaka et al., 2005). For example, the regionally extensive Vastitas interior and marginal units (units A_{BV_i} and A_{BV_m}, respectively), are interpreted to be sediments from outflow channels and perhaps other sources along the highland margin, possibly emplaced originally within ocean or as mass flows during Late Hesperian, coincident with Chryse outflow-channel dissection (for detailed spatial and temporal geologic information, as well as interpretation, please see the geologic map of Tanaka et al., 2005, which is largely based on post-Viking information acquired from the MGS and Odyssey spacecrafts). Other map units include the Isidis unit (unit A_{Ii}), which covers most of Isidis Planitia and shares similar morphologic features with the Vastitas units, and the Utopia 1 and 2 units (units H_{BU_1} and H_{BU_1}), which are interpreted to be clastic material derived from collapse, erosion, transport, and deposition of highland Noachian materials, perhaps by volatile-assisted slope processes (Tanaka et al., 2005). On the other hand, relatively low Fe concentrations (similar to K and Th) correspond with lava flows and construct-forming materials such as distinct in the region which includes the southwest flank of Arsia Mons (e.g., Karunatillake et al., 2007), volcanic materials which may include both pyroclastics and lava flows (Keszthelyi et al., 2008).

Boynton et al. (2007) suggest that the cause of the apparent Fe enrichment in the northern lowlands may be due to aqueous processes, including weathering. Outcrops of jarosite identified by the Opportunity rover in a reportedly ancient (e.g., Noachian) aqueous environment at Meridiani Planum, Mars (Squyres et al., 2004), possibly shallow submarine (Fairén et al., 2003), yield clues to the aqueous environmental conditions at a time when major magmatic-driven activity (Dohm et al., 2001a, 2007b) and/or exogenic-driven activity related to major impact events may have been occurring during the period of late heavy bombardment (e.g., Segura et al., 2002). If there were aqueous conditions, especially driven by endogenic-driven activity or exogenic-driven activity, then is it possible that a record of weathering, leaching, and erosion of iron-enriched rocks and paleosols and subsequent transport and eventually deposition into the catchment region of the northern plains would persist through subsequent diverse geologic phenomena (e.g., Tanaka et al., 2005)?

To address this important query, we rely on terrestrial field-based information. For example, in addition to field investigations that have revealed mining-related acidic aqueous conditions and associated leaching of Fe (e.g., Wai et al., 1980; Fernández-Remolar et al., 2004), investigations have also shown possible linkages between natural lacustrine and fluvial environments, materials of surrounding watersheds, and enrichment of Fe in the lacustrine and fluvial sediments. Examples include: (1) Lake Matoaka where Fe is typically higher in the sediments located in the deepest part of the lake and strongly correlated with phosphorous (P) concentration rather than other elements such as Si, carbon (C), or nitrogen (N) (Pensa and Chambers, 2004); (2) Lake Baikal where massive sedimentary layers are enriched in Fe and Mn, particularly identified within the upper 15–25 cm of sediments exclusively in the northern part of the lake, which are characterized by low sedimentation rates and deep sulfate penetration depth in the pore waters (Granina et al., 2004); (3) paleosols and paleoenvironments of the middle Miocene, Maboko Formation, Kenya, where iron–manganese nodules (Yom pedotype) are likened to modern soils of seasonally waterlogged depressions (dambo) (Retallack et al., 2002); (4) paleoenvironments of the latest Cretaceous dinosaurs of Romania where fluvial deposits and paleosols of the Transylvanian and hateg basins show three formations which are characterized by the presence of carbonate nodules closely associated with ion oxides, rhizocretions, and slickenside; here intergrowth of carbonate nodules and iron oxides is common in soils formed in a climatic regime characterized by alternating wet and dry cycles, as carbonate

precipitates under dry conditions while iron oxides are mobile under reduced soil conditions (Therrien, 2005); (5) the Bighorn Basin where two kinds of cumulative floodplain paleosols (red and purple) formed on overbank Paleogene deposits of the Willwood Formation; whereas the red paleosols result from hematite, which is commonly associated with well-drained conditions and is favored by subtrophic climate with a marked dry season, the intense mottling and presence of iron-oxide nodules in the purple paleosols are characteristics of poorly drained soils (Kraus and Gwinn, 1997); (6) the volcanogenic lake Laguna Potrok Aike, Santa Cruz, Argentina, where a depth profile of geochemical proxies of 100 cm reveals an unprecedented continuous high-resolution climatic record for the steppe regions of southern Patagonia, including rapid climatic changes before the turn of the first millennium followed by medieval droughts which are intersected by moist and/or cold periods of varying durations and intensities; the depth profiles of Fe and K resemble each other when compared to other chemical proxies (Haberzettl et al., 2005).

While igneous processes most likely contributed to the GRS-based signatures, such as hypothesized through detailed K/Th-based investigations (Taylor et al. (2006a, b) and Karunatillake et al. (2006)), as well as observed at the volcanic provinces where elemental abundances are generally low (Fig. 6), it is argued that marine, lacustrine, and fluvial rock materials and related aqueous environmental conditions as earlier discussed also contribute significantly to the signatures. As such, multiple processes are recorded in the evolutional history of Mars, not having been totally obscured by more late-stage processes such as wind-driven mantling of fine-grained basaltic materials during extended periods of ice house conditions (Baker, 2001; Baker et al., 2007). Such a hypothesized history, based in part on terrestrial field investigations, lends itself to a set of specific, powerful, and testable predictions, among them being wide lateral and vertical zonation of clastic and chemical mineral facies throughout the northern plains, similar to catchment basins on Earth.

6. Conclusions

Based on a comparison among MGS–TES, Pathfinder, and Viking IRTM datasets, the elemental distribution on Mars may be explained by inherent variations in igneous rocks and by variations in the extent and type of aqueous alteration (Taylor et al., 2006a, b; Karunatillake et al., 2006). On the other hand, when coupled with other lines of evidence, which includes Viking data and recent results from the MOLA instrument of Mars Global Surveyor, GRS elemental information is consistent with the paleohydrologic activity documented in the literature, such as the transferal of volatiles and rock materials to the northern plains and the formation of lakes and oceans in the northern plains, which includes paleosols and lacustrine and marine deposits that either remained unburied and/or are exposed by erosion and deformation. Importantly, the hypotheses illustrated above may not be mutually exclusive, as recent findings are revealing a complex geological history, similar in many respects to that of the Earth. GRS is a unique data set as it sees through $\frac{1}{3}$ m, including the thin veneer observed by spectral imagers. GRS observes the near-surface/surface conditions of the northern plains, which turns out to be heterogeneous, consistent with geologic investigations of the northern plains that show diverse geology. This diversity may include: (1) lava flows, (2) perigalcially modified rocks, which may include thick lenses of ice and fine-grained materials, (3) aeolian deposits, (4) debris flow materials, (5) remnant rock materials derived from the break up and modification of the highland–lowland boundary through time (including marine and lacustrine deposits), (6) fluvial deposits stemming from both outflow activity and spring-fed activity, (7) volcanic airfall material from both Tharsis and Elysium, (8) lahar material debouched into the Utopia basin, (9) volatile-release materials from subterranean gaseous releases and sedimentary volcanism related to fluid overpressure (e.g., mud volcanoes), (10) glacially deposited rocks, such as those sourcing from Olympus Mons and the Tharsis Montes volcanoes, (11) ice of buried glaciers and ice sheets, including expanses of formerly more extended polar caps, and (12) lacustrine and marine sediments in the basins of the northern plains. This investigation indicates that the latter (12) is a viable part of the paleohydrological history of Mars.

Further investigations are necessary to answer the enduring debate of whether oceans occupied Mars, which include using recently acquired and yet-to-be-released information. For example, once finalized, additional GRS map information such as calcium and aluminum will add additional insight. Other perspectives that will likely have a bearing on the ongoing oceans' debate include existing and yet-to-be-released remote sensing information provided by the instruments onboard the Mars orbiters, as well as rovers such as the Mars Exploration Rover, Opportunity. The Mars Reconnaissance Orbiter (MRO) includes the High Resolution Imaging Science Experiment (HIRISE), which provides detailed images (0.25–1.3 m/pixel) (McEwen et al., 2007), and the Compact Reconnaissance Imaging Spectrometer (CRISM) for Mars, which images a region approximately $10 \times 10\,km^2$ at full spatial resolution (15–19 m/pixel) and spectral resolution (544 channels covering 362–3920 nm) (Murchie et al., 2007). Both may provide geological context for the aqueous conditions presented here, although even HIRISE may not have sufficient resolution to explore any exposed paleoocean-boundary stratigraphy (e.g., wave facies). Additionally, radar-based reconnaissance of the Martian surface may also provide significant information. For example, the Shallow Subsurface Radar (SHARAD) will probe the subsurface using radar waves with a 15–25 MHz frequency band in order to get the desired high depth resolution (compared to 1.3–5.5 MHz range of MARSIS (Seu et al., 2007). The radar wave return, which is captured by the SHARAD antenna, is sensitive to changes in the dielectric properties of the coarse- and fine-grain materials such as rock and sand, respectively, and surface and subsurface water (e.g., Nunes and Phillips, 2006). Similar to high-density rock, water is an excellent conductor, and thus will have a strong radar return. Changes in the reflection characteristics of the subsurface, such as layered deposits, would also be visible as evident in the promising preliminary investigations by Phillips et al. (2007). The Phoenix Mars Mission also has elevated potential to yield significant clues to the environmental past.

Acknowledgments

We are grateful to the Gamma Ray Spectrometer team whose diligent efforts have yielded tremendous fruit. Kyeong Kim is partially supported by the Basic Research Project (08-3611) of the Korea Institute of Geoscience and Mineral Resources (KIGAM) funded by the Ministry of Science and Technology (MOST) of Korea. We are grateful to Richard Soare and an anonymous reviewer for their thoughtful reviews, all of which resulted in a significantly improved manuscript.

References

Acuña, M.H., Connerney, J.E.P., Ness, N.F., Lin, R.P., Mitchell, D., Carlson, C.W., Mcfadden, J., Anderson, K.A., Reme, H., Mazelle, C., Vignes, D., Wasilewski, P., Cloutier, P., 1999. Global distribution of crustal magnetization discovered by the Mars global surveyor MAG/ER experiment. Science 284, 790–793.

Acuña, M.H., Connerney, J.E.P., Wasilewski, P., Lin, R.P., Mitchell, D., Anderson, K.A., Carlson, C.W., McFadden, J., Réme, H., Mazelle, C., Vignes, D., Bauer, S.J.,

Cloutier, P., Ness, N.F., 2001. Magnetic field of Mars: summary of results from the aerobraking and mapping orbits. J. Geophys. Res. 106, 23403–23417.
Anderson, R.C., Dohm, J.M., Golombek, M.P., Haldemann, A., Franklin, B.J., Tanaka, K.L., Lias, J., Peer, B., 2001. Significant centers of tectonic activity through time for the western hemisphere of Mars. J. Geophys. Res. 106, 20563–20585.
Anderson, R.C., Dohm, J.M., Haldemann, A.F.C., Hare, T.M., Baker, V.R., 2004. Tectonic histories between Alba Patera and Syria Planum, Mars. Icarus 171, 31–38.
Arkani-Hamed, J., 2003. Thermoremanent magnetization of the Martian lithosphere. J. Geophys. Res. 108.
Arkani-Hamed, J., 2004. Timing of the Martian core dynamo. J. Geophys. Res. 109.
Baker, V.R., 2001. Water and the martian landscape. Nature 412, 228–236.
Baker, V.R., Strom, R.G., Gulick, V.C., Kargel, J.S., Komatsu, G., Kale, V.S., 1991. Ancient oceans, ice sheets and the hydrological cycle on Mars. Nature 352, 589–594.
Baker, V.R., Strom, R.G., Dohm, J.M., Gulick, V.C., Kargel, J.S., Komatsu, G., Ori, G.G., Rice, J.W., 2000. Mars' Oceanus Borealis, ancient glaciers, and the MEGAOUTFLO hypothesis. Lunar Planetary Science Conference, XXXI, #1863 (abstract) [CD-ROM].
Baker, V.R., Maruyama, S., Dohm, J.M., 2002. A theory of plate tectonics and subsequent long-term superplume activity on Mars, in international workshop: role of superplumes in the earth system. Electronic Geosci., 312–316.
Baker, V.R., Maruyama, S., Dohm, J.M., 2007. Tharsis superplume and the geological evolution of early Mars. In: Yuen, D.A., Maruyama, S., Karato, S.-I., Windley, B.F. (Eds.), Superplumes: Beyond Plate Tectonics. Springer, Berlin, pp. 507–523.
Bibring, J.-P., Langevin, Y., Mustard, J.F., Poulet, F., Arvidson, R., Gendrin, A., Gondet, B., Mangold, N., Pinet, P., Forget, F., The OMEGA Team, Berthe, M., Bibring, J.-P., Gendrin, A., Gomez, C., Gondet, B., Jouglet, D., Poulet, F., Soufflot, A., Vincendon, M., Combes, M., Drossart, P., Encrenaz, T., Fouchet, T., Merchiorri, R., Belluci, G., Altieri, F., Formisano, V., Capaccioni, F., Cerroni, P., Coradini, A., Fonti, S., Korablev, O., Kottsov, V., Ignatiev, N., Moroz, V., Titov, D., Zasova, L., Loiseau, D., Mangold, N., Pinet, P., Doute, S., Schmitt, B., Sotin, C., Hauber, E., Hoffmann, H., Jaumann, R., Keller, U., Arvidson, R., Mustard, J.F., Duxbury, T., Forget, F., Neukum, G., 2006. Global mineralogical and aqueous Mars history derived from OMEGA/Mars express data. Science 312, 400–404.
Birkeland, P.W., 1999. Soils and Geomorphology. Oxford U. Press, Oxford, UK, p. 95.
Boynton, W.V., Feldman, W.C., Squyres, S.W., Prettyman, T., Brückner, J., Evans, L.G., Reedy, R.C., Starr, R., Arnold, J.R., Drake, D.M., Englert, P.A.J., Metzger, A.E., Mitrofanov, I., Trombka, J.I., d'Uston, C., Wänke, H., Gasnault, O., Hamara, D.K., Janes, D.M., Marcialis, R.L., Maurice, S., Mikheeva, I., Taylor, G.J., Tokar, R., Shinohara, C., 2002. Distribution of hydrogen in the near-surface of Mars: evidence for subsurface ice deposits. Science 297, 81–85.
Boynton, W.V., Feldman, W.C., Mitrofanov, I., Evans, L.G., Reedy, R.C., Squyres, S.W., Starr, R., Trombka, J.I., d'Uston, C., Arnold, J.R., Englert, P.A.J., Metzger, A.E., Wänke, H., Brückner, J., Drake, D.M., Shinohara, C., Fellows, C., Hamara, D.K., Harshman, K., Kerry, K., Turner, C., Ward, M., Barthe, H., Fuller, K.R., Storms, S.A., Thornton, G.W., Longmire, J.L., Litvak, M.L., Ton'Chev, A.K., 2004. The Mars Odyssey gamma-ray spectrometer instrument suite. Space Sci. Rev. 110, 37–83.
Boynton, W.V., et al., 2007. Concentration of H, Si, Cl, K, Fe, and Th in the low- and mid-latitude regions of Mars. J. Geophys. Res. 112, E12S99.
Burr, D.M., Grier, J.A., McEwen, A.S., Keszthelyi, L.P., 2002. Repeated aqueous flooding from the Cerberus Fossae: evidence for very recently extant, deep groundwater on Mars. Icarus 159, 53–73.
Cabrol, N.A., Wynn-Williams, D.D., Crawford, D.A., Grin, E.A., 2001. Recent aqueous environments in Martian impact craters: an astrobiological perspective. Icarus 154, 98–113.
Carr, M.H., 1990. D/H on Mars: the effect of floods, volcanism, impacts and polar processes. Icarus 87, 210–227.
Carr, M.H., 2002. Elevations of water-worn features on Mars: implications for circulation of groundwater. J. Geophys. Res. 107, 5131.
Carr, M.H., Head, J.W., 2003. Oceans on Mars: an assessment of the observational evidence and possible fate. J. Geophys. Res. 108 (E5), 5042.
Chan, M.A., Beitler, B., Parry, W.T., Ormö, J., Komatsu, G., 2004. A possible terrestrial analogue for haematite concretions on Mars. Nature 429, 731–734.
Clifford, S.M., Parker, T.J., 2001. The evolution of the Martian hydrosphere: implications for the fate of a primordial ocean and the current state of the northern plains. Icarus 154, 40–79.
Connerney, J.E.P., Acuña, M.H., Wasilewski, P.J., Kletetschka, G., Ness, N.F., Rème, H., Lin, R.P., Mitchell, D.L., 1999. The global magnetic field of Mars and implications for crustal evolution. Science 284, 790–793.
Connerney, J.E.P., Acuña, M.H., Ness, N.F., Kletetschka, G., Mitchell, D.L., Lin, R.P., Reme, H., 2005. Tectonic implications of Mars crustal magnetism, In: Proceedings of the National Academy of Sciences of the USA (PNAS), 102, pp. 14970–14975.
Crown, D.A., Price, K.H., Greeley, R., 1992. Geologic evolution of the east rim of the Hellas basin, Mars. Icarus 100, 1–25.
Dohm, J.M., Ferris, J.C., Baker, V.R., Anderson, R.C., Hare, T.M., Strom, R.G., Barlow, N.G., Tanaka, K.L., Klemaszewski, J.E., Scott, D.H., 2001a. Ancient drainage basin of the Tharsis region, Mars: potential source for outflow channel systems and putative oceans or paleolakes. J. Geophys. Res. 106, 32943–32958.
Dohm, J.M., Anderson, R.C., Baker, V.R., Ferris, J.C., Rudd, L.P., Hare, T.M., Rice Jr., J.W., Casavant, R.R., Strom, R.G., Zimbelman, J.R., Scott, D.H., 2001b. Latent outflow activity for western Tharsis, Mars: significant flood record exposed. J. Geophys. Res. 106, 12301–12314.
Dohm, J.M., Tanaka, K.L., Hare, T.M., 2001c. Geologic map of the Thaumasia region of Mars. USGS Misc. Inv. Ser. (Map I-2650, scale 1:5,000,000).
Dohm, J.M., Maruyama, S., Baker, V.R., Anderson, R.C., Ferris, J.C., Hare, T.M., 2002. Plate tectonism on early Mars: Diverse geological and geophysical evidence. Lunar Planetary Sciience Conference XXXIII, #1639 (abstract) [CD-ROM].
Dohm, J.M., Ferris, J.C., Barlow, N.G., Baker, V.R., Mahaney, W.C., Anderson, R.C., Hare, T.M., 2004. The northwestern slope valleys (NSVs) region, Mars: a prime candidate site for the future exploration of Mars. Planet. Space Sci. 52, 189–198.
Dohm, J.M., Kerry, K., Keller, J.M., Baker, V.R., Maruyama, S., Anderson, R.C., Ferris, J.C., Hare, T.M., 2005. Mars geological province designations for the interpretation of GRS data. Lunar Planetary Science Conference XXXVI, #1567 (abstract) [CD-ROM].
Dohm, J.M., Barlow, N.G., Anderson, R.C., Williams, J.-P., Miyamoto, H., Ferris, J.C., Strom, R.G., Taylor, G.J., Fairén, A.G., Baker, V.R., Boynton, W.V., Keller, J.M., Kerry, K., Janes, D., Rodríguez, A., Hare, T.M., 2007a. Possible ancient giant basin and related water enrichment in the Arabia Terra province, Mars. Icarus.
Dohm, J.M., Baker, V.R., Maruyama, S., Anderson, R.C., 2007b. Traits and evolution of the Tharsis superplume, Mars. In: Yuen, D.A., Maruyama, S., Karato, S.-I., Windley, B.F. (Eds.), Superplumes: Beyond Plate Tectonics. Springer, Berlin, pp. 523–537.
Dohm, J.M., Baker, V.R., Boynton, W.V., Fairén, A.G., Kargel, J.S., Karunatillake, S., Keller, J., Schulze-Makuch, D., 2007c. Recent geological and hydrological activity on Mars: the Tharsis/Elysium corridor. Lunar Planetary Science Conference XXXVIII, #1686 (abstract) [CD-ROM].
Dohm, J.M., Anderson, R.C., Barlow, N.G., Miyamoto, H., Davies, A.G., Taylor, G.J., Baker, V.R., Boynton, W.V., Keller, J., Kerry, K., Janes, D., Fairén, A.G., Schulze-Makuch, D., Glamoclija, M., Marinangeli, L., Ori, G.G., Strom, R.G., Williams, J-P., Ferris, J.C., Rodíguez, J.A.P., de Pablo, M.A., Karunatillake, S., 2008. Recent geological and hydrological activity on Mars: the Tharsis/Elysium corridor. Planet. Space Sci. 56, 985–1013.
Edgett, K.S., 2005. The sedimentary rocks of Sinus Meridiani: five key observations from data acquired by the Mars global surveyor and Mars Odyssey orbiters. Mars 1, 5–58.
Edgett, K.S., Malin, M.C., 2002. Martian sedimentary rock stratigraphy: outcrops and interbedded craters of northwest Sinus Meridiani and southwest Arabia Terra. Geophys. Res. Lett. 29.
Edgett, K.S., Parker, T.J., 1997. Water on early Mars: possible subaqueous sedimentary deposits covering ancient cratered terrain in western Arabia and Sinus Meridiani. Geophys. Res. Lett. 24, 2897–2900.
Fagents, S.A., Lanagan, P., Greeley, R., 2002. Rootless cones on Mars: a consequence of lava–ground ice interaction. In: Smellie, J.L., Chapman, M.G. (Eds.), Volcano–Ice Interaction on Earth and Mars, Vol. 202. Geol. Soc. Spec. Publ., Geological Society of London, Bath, UK, pp. 295–317.
Fairén, A.G., Dohm, J.M., 2004. Age and origin of the lowlands of Mars. Icarus 168, 277–284.
Fairén, A.G., Ruiz, J., Anguita, F., 2002. An origin for the linear magnetic anomalies on Mars through accretion of terranes: implications for dynamo timing. Icarus 160, 220–223.
Fairén, A.G., Dohm, J.M., Baker, V.R., de Pablo, M.A., Ruiz, J., Ferris, J.C., Anderson, R.C., 2003. Episodic flood inundations of the northern plains of Mars. Icarus 165, 53–67.
Fairén, A.G., Fernández-Remolar, D., Dohm, J.M., Baker, V.R., Amils, R., 2004. Inhibition of carbonate synthesis in acidic oceans on early Mars. Nature 431, 423–426.
Feldman, W.C., Boynton, W.V., Tokar, R.L., Prettyman, T.H., Gasnault, O., Squyres, S.W., Elphic, R.C., Lawrence, D.J., Lawson, S.L., Maurice, S., McKinney, G.W., Moore, K.R., Reedy, R.C., 2002. Global distribution of neutrons from Mars: results from Mars odyssey. Science 297, 75–78.
Feldman, W.C., Prettyman, T.H., Maurice, S., Plaut, J.J., Bish, D.L., Vaniman, D.T., Mellon, M.T., Metzger, A.E., Squyres, S.W., Karunatillake, S., Boynton, W.V., Elphic, R.C., Funsten, H.O., Lawrence, D.J., Tokar, R.L., 2004. Global distribution of near-surface hydrogen on Mars. J. Geophysical Res. Planets 109 (E9), E09006.
Feldman, W.C., Prettyman, T.H., Maurice, S., Nelli, S., Elphic, R., Funsten, H.O., Gasnault, O., Lawrence, D.J., Murphy, J.R., Tokar, R.L., Vaniman, D.T., 2005. Topographic control of hydrogen deposits at low latitudes to midlatitudes of Mars. J. Geophysical Res. Planets 110 (E11), E11009.
Fernández-Remolar, D., Gómez-Elvira, J., Gómez, F., Sebastian, E., Martíin, J., Manfredi, J.A., Torres, J., González Kesler, C., Amils, R., 2004. The Tinto river, an extreme acidic environment under control of iron, as an analog of the Terra Meridiani hematite site of Mars. Planet. Space Sci. 52, 239–248.
Ferris, J.C., Dohm, J.M., Baker, V.R., Maddock, T., 2002. Dark slope streaks on Mars: are aqueous processes involved? Geoph. Res. Lett. 29.
Fialips, C.I., Carey, J.W., Vaniman, D.T., Bish, D.L., Feldman, W.C., Mellon, M.T., 2005. Hydration state of zeolites, clays, and hydrated salts under present-day Martian surface conditions: can hydrous minerals account for Mars Odyssey observations of near-equatorial water-equivalent hydrogen? Icarus 178, 74–83.
Forget, F., Haberle, R.M., Montmessin, F., Levrard, B., Head, J.W., 2006. Formation of glaciers on Mars by atmospheric precipitation at high obliquity. Science 311, 368–371.
Gendrin, A., Mangold, N., Bibring, J.P., Langevin, Y., Gondet, B., Poulet, F., Bonello, G., Quantin, C., Mustard, J., Arvidson, R., LeMouelic, S., 2005. Sulfates in Martian layered terrains: the OMEGA/Mars express view. Science 307, 1587–1591.
Ghatan, G.J., Zimbelman, J.R., 2006. Paucity of candidate coastal constructional landforms along proposed shorelines on Mars: Implications for a northern lowlands-filling ocean. Icarus 185, 171–196.

Goldspiel, J.M., Squyres, S.W., 1991. Ancient aqueous sedimentation on Mars. Icarus 89, 392–410.
Granina, L., Müller, B., Wehrli, B., 2004. Origin and dynamics of Fe and Mn sedimentary layers in Lake Baikal. Chem. Geol. 205, 55–72.
Greeley, R., Guest, J.E., 1987. Geologic map of the eastern equatorial region of Mars. USGS Misc. Inv. Ser. (Map I-1802B, (1:15,000,000)).
Greenwood, J.P., Blake, R.E., 2006. Evidence for an acidic ocean on Mars from phosphorus geochemistry of Martian soils and rocks. Geol. Soc. Am. 34, 953–956.
Grotzinger, J.P., Bell III, J.F., Calvin, W., Clark, B.C., Fike, D.A., Golombek, M., Greeley, R., Herkenhoff, K.E., Jolliff, B., Knoll, A.H., Malin, M., McLennan, S.M., Parker, T., Soderblom, L., Sohl-Dickstein, J.N., Squyres, S.W., Tosca, N.J., Watters, W.A., 2005. Stratigraphy, sedimentology and depositional environment of the Burns Formation, Meridiani Planum, Mars. Earth Planet. Sci. Lett. 240, 11–72.
Gulick, V.C., Baker, V.R., 1990. Origin and evolution of valleys on Martian volcanoes. J. Geophys. Res. 95, 14325–14334.
Haberzettl, T., Fey, M., Lücke, A., Maidana, N., Mayr, C., Ohlendorf, C., Schäbitz, F., Schleser, G.H., Wille, M., Zolitschka, Bernd, 2005. Climatically induced lake level changes during the last two millennia as reflected in sediments of Laguna Potrok Aike, southern Patagonia (Santa Cruz, Argentina). J. Paleolimnol. 33, 283–302.
Hahn, B.C., McLennan, S.M., Taylor, G.J., Boynton, W.V., Dohm, J.M., Finch, M.J., Hamara, D.K., Janes, D.M., Karunatillake, S., Keller, J.M., Kerry, K.E., Metzger, A.E., Williams, R.M.S., 2007. Mars Odyssey gamma ray spectrometer elemental abundances and apparent relative surface age: implications for Martian crustal evolution. J. Geophys. Res. 112, E03S11.
Head, J.W., Pratt, S., 2001. Extensive Hesperian-aged south polar ice sheet on Mars: evidence for massive melting and retreat, and lateral flow and ponding of meltwater. J. Geophys. Res. 106, 12275–12299.
Head, J.W., Kreslavsky, M., Hiesinger, H., Ivanov, M.A., Pratt, S., Seibert, N., Smith, D.E., Zuber, M.T., 1998. Oceans in the past history of Mars: test for their presence using Mars orbiter laser altimeter (MOLA) data. Geophys. Res. Lett. 25, 4401–4404.
Head, J.W., Hiesinger, H., Ivanov, M.A., Krelavshky, M.A., Pratt, S., Thomson, B.J., 1999. Possible ancient oceans on Mars: evidence from Mars orbiter laser altimeter data. Science 286, 2134–2137.
Head, J.W., Kreslavsky, M.A., Pratt, S., 2002. Northern lowlands on Mars: evidence for widespread volcanic flooding and tectonic deformation in the Hesperian period. J. Geophys. Res. 107, 8.
Head, J.W., Mustard, J.F., Kreslavsky, M.A., Milliken, R.E., Marchant, D.R., 2003. Recent ice ages on Mars. Nature 426, 797–802.
Head, J.W., Marchant, D.R., Agnew, M.C., Fassett, C.I., Kreslavsky, M.A., 2006a. Extensive valley glacier deposits in the northern mid-latitudes of Mars: evidence for late Amazonian obliquity-driven climate change. Earth Planet. Sci. Lett. 241, 663–671.
Head, J.W., Nahm, A.L., Marchant, D.R., Neukum, G., 2006b. Modification of the dichotomy boundary on Mars by Amazonian mid-latitude regional glaciation. Geophy. Res. Lett. 33.
Hodges, C.A., Moore, H.J., 1994. Atlas of Volcanic Landforms on Mars. US Geol. Surv. Prof. Pap. 1534, 194.
Ivanov, M.A., Head, J.W., 2001. Chryse Planitia, Mars: topographic configuration, outflow channel continuity and sequence, and tests for hypothesized ancient bodies of water using Mars orbiter laser altimeter (MOLA) data. J. Geophys. Res. 106, 3275–3295.
Jöns, H.P., 1986. Arcuate ground undulations, gelifluxion-like features and "front tori" in the northern lowlands on Mars. What do they indicate? Lunar Planetary Science Conference, XVII, # 404-405 (abstract) [CD-ROM].
Kargel, J.S., 2004. Mars: A Warmer Wetter Planet. Praxis-Springer, p. 557.
Kargel, J.S., Strom, R.G., 1992. Ancient glaciation on Mars. Geology 20, 3–7.
Kargel, J.S., Baker, V.R., Beget, J.E., Lockwood, J.F., Pewe, T.L., Shaw, J.S., Strom, R.G., 1995. Evidence of ancient continental glaciation in the Martian northern plains. J. Geophys. Res. 100, 5351–5368.
Karunatillake, et al., 2008. Recipes for spatial statistics with global datasets: A Martian case study, in preparation.
Karunatillake, S.K., Squyres, S.W., Taylor, G.J., Keller, J., Gasnault, O., Evans, L.G., Reedy, R.C., Starr, R., Boynton, W., Janes, D.M., Kerry, K., Dohm, J.M., Sprague, A.L., Hamara, D., 2006. Composition of northern low-albedo regions of Mars: insights from the Mars Odyssey gamma ray spectrometer. J. Geophys. Res. 111, E03S05.
Karunatillake, S.K., Squyres, S.W., Taylor, G.J., McLennan, S., Boynton, W.V., 2007. Chemically striking regions on Mars revealed by the Mars Odyssey Gamma Ray Spectrometer. Abstract present at the Seventh International Conference on Mars.
Keller, J., Boynton, W.V., Baker, V.R., Dohm, J.M., Evans, L.G., Hamara, D., Janes, D., Karunatillake, S., Kerry, K., Reedy, R.C., Squyres, S.W., Starr, R.D., Taylor, J., The GRS Team, 2006. Equatorial and midlatitude distribution of chlorine measured by Mars Odyssey GRS. J. Geophys. Res. 111, E03S08.
Keszthelyi, L., Jaeger, W., McEwen, A., Tornabene, L., Beyer, R.A., Dundas, C., Milazzo, M., 2008. High Resolution Imaging Science Experiment (HiRISE) images of volcanic terrains from the first 6 months of the Mars Reconnaissance Orbiter Primary Science Phase. J. Geophys. Res. 113, E04005.
Komatsu, G., Ori, G.G., Marinangeli, L., Moersch, J.E., 2007. Playa environments on Earth: possible analogues for Mars. In: Chapman, M.G. (Ed.), The Geology of Mars: Evidence from Earth-Based Analogs. Cambridge University Press, Cambridge, pp. 322–348.
Konopliv, A., Yoder, C., Standish, E., Yuan, D.-N., Sjogren, W., 2006. A global solution for the Mars static and seasonal gravity, Mars orientation, Phobos and Deimos masss, and Mars ephemerides. Icarus 182, 23–50.
Kostama, V.P., Kreslavsky, M.A., Head, J.W., 2006. Recent high-latitude icy mantle in the northern plains of Mars: characteristics and ages of emplacement. Geophys. Res. Lett. 33.
Kraus, M.J., Gwinn, B., 1997. Facies and facies architecture of Paleogenie floodplain deposits, Willwood Formation, Bighorn Basin, Wyoming, USA. Sediment. Geol. 114, 33–54.
Kreslavsky, M.A., Head, J.W., 2002. Fate of outflow channel effluents in the northern lowlands of Mars: the Vastitas Borealis Formation as a sublimation residue from frozen ponded bodies of water. J. Geophys. Res. 107 (E12), 5121.
Lanagan, P.D., McEwen, A.S., Keszthelyi, L.P., Thordarson, T., 2001. Rootless cones on Mars indicating the presence of shallow equatorial ground ice in recent times. Geophys. Res. Lett. 28, 2365–2368.
Laskar, J., Robutel, P., 1993. The chaotic obliquity of the planets. Nature 361, 608–612.
Leonard, G.J., Tanaka, K.L., 2001. Geologic map of the Hellas region of Mars. US Geol. Surv. Geol. Inv. Ser. (Map I-2694).
Leverington, D.W., Ghent, R.R., 2004. Differential subsidence and rebound in response to changes in water loading on Mars: possible effects on the geometry of ancient shorelines. J. Geophys. Res. 109, E01005.
Litvak, M.L., Mitrofanov, I.G., Kozyrev, A.S., Sanin, A.B., Tretyakov, V.I., Boynton, W.V., Kelly, N.J., Hamara, D., Shinohara, C., Saunders, R.S., 2006. Comparison between polar regions of Mars from HEND/Odyssey data. Icarus 180 (1), 23–27.
López, V., Tejero, R., Ruiz, J., Gómez-Ortiz, D., 2006. The elevation range of the possible Meridiani/Arabia Paleoshoreline, Mars. Lunar Planetary Science [CD-ROM], XXXVII, abstract 1810.
Lucchitta, B.K., Ferguson, H.M., Summers, C., 1986. Sedimentary deposits in the northern lowland plains, Mars. J. Geophys. Res. 91, E166–E174.
Mahaney, W.C., Dohm, J.M., Baker, V.R., et al., 2001. Morphogenesis of Antarctic paleosols: Martian analogue. Icarus 154, 113–130.
Malin, M.C., Edgett, K.S., 1999. Oceans or seas in the Martian northern lowlands: High resolution imaging tests of proposed coastlines. J. Geophys. Res. Lett. 26, 3049–3052.
Malin, M.C., Edgett, K.S., 2000. Sedimentary rocks of early Mars. Science 290, 1927–1937.
Malin, M.C., Edgett, K.S., 2001. Mars global surveyor Mars orbiter camera: interplanetary cruise through primary mission. J. Geophys. Res. 106 (E10), 23429–23570.
Malin, M.C., Edgett, K.S., 2003. Evidence for persistent flow and aqueous sedimentation on early Mars. Science 302, 1931–1934.
Malin, M.C., Edgett, K.S., Posiolova, L.V., McColley, S.M., Noe Dobrea, E.Z., 2006. Present-day impact cratering rate and contemporary gully activity on Mars. Science 314, 1573–1577.
McEwen, et al., 2007. Mars reconnaissance orbiter's high resolution imaging science experiment (HiRISE). J. Geophys. Res. 112.
McGovern, P.J., Solomon, S.C., Smith, D.E., Zuber, M.T., Simons, M., Wieczorek, M.A., Phillips, R.J., Neumann, G.A., Aharonson, O., Head, J.W., 2002. Localized gravity/topography admittance and correlation spectra on Mars: implications for regional and global evolution. J. Geophys. Res. 107, 5136.
McGovern, P.J., Solomon, S.C., Smith, D.E., Zuber, M.T., Simons, M., Wieczorek, M.A., Phillips, R.J., Neumann, G.A., Aharonson, O., Head, J.W., 2004. Correction to localized gravity/topography admittance and correlation spectra on Mars: implications for regional and global evolution. J. Geophys. Res. 109, E07007.
Ming, D.W., et al., 2006. Geochemical and mineralogical indicators for aqueous processes in the Columbia Hills of Gusev crater, Mars. J. Geophys. Res. 111, E02S12.
Mitrofanov, I., Anfimov, D., Kozyrev, A., Litvak, M., Sanin, A., Tret'yakov, V., Krylov, A., Shvetsov, V., Boynton, W., Shinohara, C., Hamara, D., Saunders, R.S., 2002. Maps of subsurface hydrogen from the high energy neutron detector, Mars Odyssey. Science 297, 78–81.
Mitrofanov, I.G., Litvak, M.L., Kozyrev, A.S., Sanin, A.B., Tret'yakov, V.I., Grin'kov, V.Yu., Boynton, W.V., Shinohara, C., Hamara, D., Saunders, R.S., 2004. Soil water content on Mars as estimated from neutron measurements by the HEND instrument onboard the 2001 Mars Odyssey spacecraft. Sol. Syst. Res. 38 (4), 253–265.
Miyamoto, H., Dohm, J.M., Beyer, R.A., Baker, V.R., 2004. Fluid dynamical implications of anastomosing slope streaks on Mars. J. Geophys. Res. 109.
Moore, J.M., Wilhelms, D.E., 2001. Hellas as a possible site of ancient ice-covered lakes on Mars. Icarus 154, 258–276.
Murchie, S., et al., 2007. Compact reconnaissance imaging spectrometer for Mars (CRISM) on Mars reconnaissance orbiter (MRO). J. Geophys. Res. 112.
Murray, J.B., Muller, J.-P., Neukum, G., Hauber, E., Markiewicz, W.J., Head, J.W., Foing, B.H., Page, D.P., Mitchell, K.L., Portyankina, G., 2005. Evidence from the Mars express high resolution stereo camera for a frozen sea close to Mars' equator. Nature 434, 352–355.
Neukum, G., Ivanov, B.A., Hartmann, W.K., 2001. Cratering records in the inner solar system in relation to the lunar reference system. In: Kallenbach, R., Geiss, J., Hartmann, W.K. (Eds.), Chronology and Evolution of Mars. Kluwer Academic Publishers, pp. 55–86.
Newsom, H.E., Crumpler, L.S., Reedy, R.C., Peterson, M.T., Newsom, G.C., Evans, L.G., Taylor, G.J., Keller, J.M., Janes, D.M., Boynton, W.V., Kerry, K.E., Karunatillake, S., 2007. Geochemistry of Martian soil and bedrock in mantled and less mantled terrains with gamma ray data from Mars Odyssey. J. Geophys. Res. 112, E03S12.

Nunes, D.C., Phillips, R.J., 2006. Radar subsurface mapping of the polar layered deposits on Mars. J. Geophys. Res. 111, E06S21.
Ori, G.G., Komatsu, G., Marinangeli, L., (Eds.), 2001. Exploring Mars surface and its terrestrial analogues, Fieldtrip guidebook 〈http://irsps.sci.unich.it/education/tunisia/index.html〉.
Ormö, Jens., Dohm, J.M., Ferris, J.C., Malvitte, A.L., Fairen, A.G., 2004a. Marine-target craters on Mars? An assessment study. Meteorit. Planet. Sci. 39, 333–346.
Ormö, J., Komatsu, G., Chan, M.A., Beitler, B., Parry, W.T., 2004b. Geological features indicative of processes related to the hematite formation in Meridiani planum and Aram Chaos, Mars: a comparison with diagenetic hematite deposits in southern Utah, USA. Icarus 171, 295–316.
Parker, T.J., Schneeberger, D.M., Pieri, D.C., Saunders, R.S., 1987. Geomorphic evidence for ancient seas on Mars. In: MECA Symposium on Mars: Evolution of its Climate and Atmosphere, LPI Technical Report 87-01, 96–98, Lunar and Planetary Institute, Houston, Tex.
Parker, T.J., Saunders, R.S., Schneeberger, D.M., 1989. Transitional morphology in the west Deuteronilus Mensae region of Mars: Implications for modification of the lowland/upland boundary. Icarus 82, 111–145.
Parker, T.J., Gorsline, D.S., Saunders, R.S., Pieri, D.C., Schneeberger, D.M., 1993. Coastal geomorphology of the Martian northern plains. J. Geophys. Res. 98, 11061–11078.
Parker, T.J., Grant, J.A., Franklin, B.J., Rice, J.W., 2001. A comparison of MOC and MOLA observations of northern plains "contacts" with coastal landforms of the Bonneville basin, Utah. Lunar Planetary Science Conference, XXXII, #2051 (abstract) [CD-ROM].
Pensa, M.A., Chambers, R.M., 2004. Trophic transition in a lake on the Virginia coastal plain. J. Environ. Qual. 33, 576–580.
Perron, J.T., Mitrovica, J.X., Manga, M., Matsuyama, I., Richards, M.A., 2007. Evidence for an ancient Martian ocean in the topography of deformed shorelines. Nature 447, 840–843.
Phillips, R.J., Seu, R., Biccari, D., Campbell, B.A., Plaut, J.J., Zuber, M.T., Murchie, S., Byrne, S., Safaeinili, A., Orosei, R., Marinangeli, L., Masdea, A., Picardi, G., Smrekar, S.E., Carter, L.M., Putzig, N.E., Nunes, D.C., SHARAD Team, 2007. North polar deposits on Mars: new insights from MARSIS, SHRAD, and other MRO instruments. Lunar Planetary Science [CD-ROM] XXXVIII, abstract 2328.
Plescia, J.B., 1990. Recent flood lavas in the Elysium region of Mars. Icarus 88, 465–490.
Press, W.H., Teukolsky, S.A., Vetterling, W.T., Flannery, B.P., 2002. Numerical Recipes in C the Art of Scientific Computing. Cambridge University Press, Cambridge, pp. 615–620.
Retallack, G.J., Wynn, J.G., Benefit, B.R., McCrossin, M.L., 2002. Paleosols and paleoenvironments of the middle Miocene, Maboko Formation, Kenya. J. Human Evol. 42, 659–703.
Rogers, A.D., Christensen, P.R., 2007. Surface mineralogy of Martian low-albedo regions from MGS-TES data: Implications for upper crustal evolution and surface alteration. J. Geophys. Res. 112, E01003.
Ruiz, J., 2003. Amplitude of heat flow variations on Mars from possible shoreline topography. J. Geophys. Res. 108 (E5), 5122.
Ruiz, J., Fairén, A.G., de Pablo, M.A., 2003. Thermal isostasy on Mars. Lunar Planetary Science [CD-ROM], XXXIV, abstract 1090.
Ruiz, J., Fairén, A.G., Dohm, J.M., Tejero, R., 2004. Thermal isostacy and deformation of possible paleoshorelines on Mars. Planet. Space Sci. 52, 1297–1301.
Ruiz, J., Tejero, R., Gomez-Ortiz, D., López, V., 2006. Paleoshorelines and the evolution of the lithosphere of Mars. In: Maravell, N.S. (Ed.), Space Science: New Research. Nova Science Publishers, Hauppauge, New York, pp. 71–96.
Schubert, G., Solomon, S.C., Turcotte, D.L., Drake, M.J., Sleep, N.H., 1992. Origin and thermal evolution of Mars. In: Kieffer, H.H., Jakosky, B.M., Snyder, C.W., Matthews, M.S. (Eds.), Mars. University of Arizona Press, Tucson, pp. 147–183.
Schulze-Makuch, D., Irwin, L.N., 2004. Life in the Universe: Expectations and Constraints. Springer, Berlin, p. 172.
Schulze-Makuch, D., Dohm, J.M., Fairén, A.G., Baker, V.R., Fink, W., Strom, R.G., 2005a. Venus, Mars, and the ices on Mercury and the Moon: astrobiological implications and proposed mission designs. Astrobiology 5, 778–795.
Schulze-Makuch, D., Irwin, L.N., Lipps, J.H., LeMone, D., Dohm, J.M., Fairén, A.G., 2005b. Scenarios for the evolution of life on Mars. J. Geophys. Res. 110, E12S23.
Scott, D.H., Chapman, M.G., 2005. Geologic and topographic maps of the Elysium Paleolake Basin, Mars. USGS Misc. Inv. Ser. (Map I-2397 (1:5,000,000)).
Scott, D.H., Dohm, J.M., 1997. Mars structural Geology and Tectonics. Encyclopedia of Planetary Sciences. Van Nostrand Reinhold, New York, pp. 461–463.
Scott, D.H., Tanaka, K.L., 1986. Geologic map of the western hemisphere of Mars; scale 1:15M. USGS Misc. Inv. Ser. (Map, I-1802-A (1:15,000,000)).
Scott, D.H., Tanaka, K.L., Greeley, R., Guest, J.E., 1986. Geologic maps of the western and eastern equatorial and polar regions of Mars. US Geol. Surv. Misc. Inv. Ser. (Map I-1802-A, B, C).
Scott, D.H., Dohm, J.M., Rice Jr., J.W., 1995. Map of Mars showing channels and possible paleolake basins. USGS Misc. Inv. Ser. (Map I-2461 (1:30,000,000)).
Segura, T.L., Toon, O.B., Colaprete, A., Zahnle, K., 2002. Environmental effects of large impacts on Mars. Science 298, 1977–1980.
Seu, R., et al., 2007. SHARAD sounding radar on the Mars reconnaissance orbiter. J. Geophys. Res. 112, E05S05.
Soare, R.J., Kargel, J.S., Osinski, G.R., Costard, F., 2007. Thermokarst processes and the origin of crater-rim gullies in Utopia and western Elysium Planitia. Icarus 191, 95–112.
Sotin, C., Couturier, F., 2007. The gravity potential along paleo-shorelines: implications for the geological history of Mars. Seventh International Conference on Mars, abstract 3404.
Squyres, S.W., Grotzinger, J.P., Arvidson, R.E., Bell III, J.F., Calvin, W., Christensen, P.R., Clark, B.C., Crisp, J.A., Farrand, W.H., Herkenhoff, K.E., Johnson, J.R., Klingelhofer, G., Knoll, A.H., McLennan, S.M., McSween Jr., H.Y., Morris, R.V., Rice Jr., J.W., Rieder, R., Soderblom, L.A., 2004. In situ evidence for an ancient aqueous environment at Meridiani Planum, Mars. Science 306, 1709–1714.
Strom, R.G., Malhotra, R., Ito, T., Yoshida, F., Kring, D.A., 2005. The origin of planetary impactors in the inner solar system. Science 309, 1847–1850.
Tanaka, K.L., 1986. The stratigraphy of Mars. Proc. Lunar Planet. Sci. Conf. 17th, Part 1. J. Geophys. Res. 91 (Suppl.), E139–E158.
Tanaka, K.L., Skinner, J.A., Hare, T.M., Joyal, T., Wenker, A., 2003. Resurfacing history of the northern plains of Mars based on geologic mapping of Mars Global Surveyor data. J. Geophys. Res. 108.
Tanaka, K.L., Skinner, J.A., Hare, T.M., 2005. Geologic map of the northern plains of Mars. USGS Miscellaneous Scientific Investigations. Map 2888, scale 1:15,000,000.
Taylor, G.J., Stopar, J., Wänke, H., Dreibus, G., Kerry, K., Keller, J., Reedy, R., Evans, L., Starr, R., Martel, L.M.V., Squyres, S., Karunatillake, S., Gasnault, O., Maurice, S., d'Uston, C., Englert, P., Dohm, J., Baker, V., Hamara, D., Janes, D., Sprague, A., Kim, K., Drake, D., 2006a. Variations in K/Th on Mars. J. Geophys. Res. 111, E03S06.
Taylor, G.J., Boynton, W., Brückner, J., Wänke, H., Dreibus, G., Kerry, K., Keller, J., Reedy, R., Evans, L., Starr, R., Squyres, S., Karunatillake, S., Gasnault, O., Maurice, S., d'Uston, C., Englert, P., Dohm, J., Baker, V., Hamara, D., Janes, D., Sprague, A., Kim, K., Drake, D., 2006b. Bulk composition and early differentiation of Mars. J. Geophys. Res. 111, E03S10.
Therrien, F., 2005. Paleoenvironments of the latest Cretaceous (Maastrichtian) dinosaurs of Romania: insight from fluvial deposits and paleosols of the Transylvanian and Hateg basins. Paleogeog., Pleoclimat., Paleoecol. 218, 15–56.
Touma, J., Wisdom, J., 1993. The chaotic obliquity of Mars. Science 259, 1294–1296.
Wai, C.M., Reece, D.E., Trexler, B.D., Ralston, D.R., Williams, R.E., 1980. Production of acid water in a lead–zinc mine, Coeur d'Alene, Idaho. Environ. Geol. 3, 159–162.